Do land surface models need to include differential plant species responses to drought? Examining model predictions across a mesic-xeric gradient in Europe.

M. G. De Kauwe[1], S.-X. Zhou[1,2], B. E. Medlyn[1,3], A. J. Pitman[4], Y.-P. Wang[5], R. A. Duursma[3] and I. C. Prentice[1,6]

[1]{Macquarie University, Department of Biological Sciences, New South Wales 2109, Australia.}

[2] {CSIRO Agriculture Flagship, Waite Campus, PMB 2, Glen Osmond, SA 5064, Australia.}

[3]{Hawkesbury Institute for the Environment, Western Sydney University, Locked Bag 1797, Penrith, NSW, Australia}

[4]{Australian Research Council Centre of Excellence for Climate Systems Science and Climate Change Research Centre, UNSW, Sydney, Austraila}

[5]{CSIRO Ocean and Atmosphere Flagship, Private Bag #1, Aspendale, Victoria 3195, Australia}

[6]{AXA Chair of Biosphere and Climate Impacts, Grand Challenges in Ecosystems and the Environment and Grantham Institute – Climate Change and the Environment, Department of Life Sciences, Imperial College London, Silwood Park Campus, Buckhurst Road, Ascot SL5 7PY, UK}

Correspondence to: M. G. De Kauwe (mdekauwe@gmail.com)

Abstract

Future climate change has the potential to increase drought in many regions of the globe, making it essential that land surface models (LSMs) used in coupled climate models, realistically capture the drought responses of vegetation. Recent data syntheses show that drought sensitivity varies considerably among plants from different climate zones, but state-of-the-art LSMs currently assume the same drought sensitivity for all vegetation. We tested whether variable drought sensitivities are needed to explain the observed large-scale patterns of drought impact on the carbon, water and energy fluxes. We implemented data-driven drought sensitivities in the Community Atmosphere Biosphere Land Exchange (CABLE) LSM and evaluated alternative sensitivities across a latitudinal gradient in Europe during the 2003 heatwave. The model predicted an overly abrupt onset of drought unless average soil water potential was calculated with dynamic weighting across soil layers. We found that high drought sensitivity at the most mesic sites, and low drought sensitivity at the most xeric sites, was necessary to accurately model responses during drought. Our results indicate that LSMs will over-estimate drought impacts in drier climates unless different sensitivity of vegetation to drought is taken into account.

1 Introduction

Changes in regional precipitation patterns with climate change are highly uncertain (Sillmann et al. 2014), but are widely expected to result in a change in the frequency, duration and severity of drought events (Allen et al. 2010). Drought is broadly defined, but for plants is a marked deficit of moisture in the root zone which results from a period of low rainfall and/or increased atmospheric demand for evapotranspiration. Recently, a series of high-profile drought events (Ciais et al. 2005; Fensham et al. 2009; Phillips et al. 2009; Lewis et al. 2011) and associated tree mortality (Breshears et al. 2005; van Mantgem et al. 2009; Peng et al. 2011; Anderegg et al. 2013), have occurred across the globe and these events have led to debate as to whether incidence of drought are increasing (Allen et al. 2010; Dai et al. 2013, but see Sheffield et al. 2012). Drought and any ensuing vegetation mortality events have the potential to change land ecosystems from a sink to source (Lewis et al. 2011), and the dominant mechanisms governing the ecosystem responses to drought can vary from reducing stomatal conductance (Xu and Baldocchi, 2003) to increasing tree mortality (Lewis et al. 2011) and changing community species composition (Nepstad et al. 2007).

Our ability to model drought effect on vegetation function (carbon and water fluxes) is currently limited (Galbraith et al. 2010; Egea et al. 2011; Powell et al. 2013). Remarkably, given the importance of correctly capturing drought impacts on carbon and water fluxes, land surface models (LSMs) designed for use in climate models have rarely been benchmarked against extreme drought events. Mahfouf et al. (1996) compared summertime crop transpiration from 14 land surface schemes, finding that only half of the models fell within the uncertainty range of the observations. They attributed differences among models to the various schemes used by models to represent transpiration processes (e.g. soil water stress function, different number of soil layers) and variability in the initial soil water content at the start of the growing season which relates to variability in the way bare soil evaporation and drainage are represented among different models. Galbraith et al. (2010) showed that a set of dynamic global vegetation models (DGVMs) were unable to capture the 20–30% reduction in biomass due to drought during a set of throughfall exclusion experiments in the Amazon. Galbraith et al. (2010) attributed model variability during drought to: changes in autotrophic respiration (which was not supported by the data), model insensitivity to observed leaf area reductions, and the use of different empirical functions to down-regulate productivity during

water stress. The models differed both in terms of time-scale of the application of this function (sub-diurnal vs. daily) and whether it was used to down-regulate net photosynthesis or the maximum rate of Rubisco activity, V_{cmax}. Similarly, Powell et al. (2013) demonstrated that a group of five models were unable to predict drought-induced reductions in aboveground biomass (~20%) in two large-scale Amazon experiments. Gerten et al. (2008) compared the effect of adjusting precipitation regimes on simulated net primary productivity (NPP) by four ecosystem models across a range of hydroclimates. They found a consistent direction of change (in terms of NPP) with different scenarios across models but found that the seasonal evolution of soil moisture differed among the models.

In order for models to better capture realistic responses during drought, they need to draw more closely on experimental data (see Chaves et al. 1993 for a review). One key observation is that there is a continuum of species responses to soil moisture deficit, ranging from isohydric (stomata close rapidly during drought, maintaining a minimum leaf water potential, Ψ_l) to anisohydric (stomata remain open during drought, which allows Ψ_l to decrease) hydraulic strategies (Tardieu and Simonneau, 1998; Klein, 2014). These differences are widely observed and are thought to be important in determining resilience to drought (McDowell et al. 2008; Mitchell et al. 2013; Garcia-Forner et al. 2015). Many traits, including hydraulic conductivity, resistance to cavitation, turgor loss point, stomatal regulation and rooting depth, contribute to these differences. Systematic differences in the response of leaf gas exchange to soil moisture potential have been observed among species originating from different hydroclimates (Zhou et al. 2013), with species from mesic environments showing stronger stomatal sensitivity to drought than species from xeric environments. Currently, these environmental gradients in species behaviour are not captured in LSMs, which typically assume static plant functional type (PFT) parameterisations. This is in part because historically the data required to describe these attributes have not been available at the global scale, but also due to the necessity of simplification required to run global climate model simulations. Species with a PFT are assumed to have similar or identical sensitivities to drought. Such an approach ignores experimental evidence of the range of sensitivities to drought among species (Choat et al. 2012; Limousin et al. 2013; Zhou et al. 2014; Mitchell et al., 2014; Mencuccini et al. 2015). For example, Turner et al. (1984) found contrasting responses in leaf water potential to increasing vapour pressure deficit, ranging from isohydric

to anisohydric, among a group of woody and herbaceous species. Similarly, Zhou et al. (2014) found that in a dry-down experiment, European sapling species originating from more mesic environments were more sensitive to water stress (more rapid reduction of photosynthesis and stomatal conductance) than species from more xeric regions. However, it is not known whether observed differences in the response to soil moisture deficit among species are important in determining fluxes at large scales.

In this study we test whether differences in species' responses to drought are needed to capture drought responses on a continental scale. We built on recent changes to the stomatal conductance (g_s) scheme (De Kauwe et al. 2015) within the Community Atmosphere Biosphere Land Exchange (CABLE) LSM (Wang et al. 2011), by implementing a new formulation for drought impacts based on plant ecophysiological studies for 31 species (Zhou et al. 2013; 2014). We obtained three parameterisations for drought response from these studies, characterising low, medium and high sensitivities to drought. We then applied CABLE to simulate responses to an extreme meteorological event, the European 2003 heatwave, at five eddy covariance sites covering a latitudinal gradient, transitioning from mesic sites at the northern extreme to xeric at the southern sites. Observations show that there was a significant impact of drought on ecosystem fluxes at these sites (Ciais et al. 2005; Schär et al. 2005). We note that models have been applied to simulate drought effects on productivity (net primary production) and leaf area at individual sites (Ciais et al. 2005; Fischer et al. 2007; Granier et al. 2007; Reichstein et al. 2007) but have not been used to examine whether alternative parameterisations are needed to capture drought responses across sites. We therefore tested how well CABLE was able to simulate the impact of drought on carbon and water fluxes at these sites using alternative parameterisations for drought sensitivity. We hypothesised that drought sensitivity would increase as sites transitioned from xeric to mesic. We hypothesised that trees at more mesic sites, with a greater abundance of available water than at xeric sites, would be more vulnerable to shorter duration droughts, and thus have higher drought sensitivity (or lower resistance to drought). Therefore, accounting for this latitudinal gradient in drought sensitivity would improve the performance of CABLE.

2 Methods

2.1 Model description

CABLE represents the vegetation using a single layer, two-leaf canopy model separated into sunlit and shaded leaves (Wang and Leuning, 1998), with a detailed treatment of within canopy turbulence (Raupach 1994; Raupach et al. 1997). Soil water and heat conduction is numerically integrated over six discrete soil layers following the Richards equation and up to three layers of snow can accumulate on the soil surface. A complete description can be found in Kowalczyk et al. (2006) and Wang et al. (2011). CABLE has been used extensively for both offline (Abramowitz et al. 2008; Wang et al. 2011; De Kauwe et al. 2015) and coupled simulations (Cruz et al. 2010; Pitman et al. 2011; Mao et al. 2011; Lorenz et al. 2014) within the Australian Community Climate Earth System Simulator (ACCESS, see http://www.accessimulator.org.au; Kowalczyk et al. 2013); a fully coupled earth system model. The source code can be accessed after registration at https://trac.nci.org.au/trac/cable.

2.2 Representing drought stress within CABLE.

We build on the work by De Kauwe et al. (2015), who introduced a new g_s scheme into CABLE. In this scheme, stomata are assumed to behave optimally; that is, stomata are regulated to maximise carbon gain whilst simultaneously minimising water loss, over short time periods (i.e. a day) (Cowan and Farquhar, 1977) leading to the following formulation of g_s (Medlyn et al. 2011)

$$g_s = g_0 + 1.6\left(1 + \frac{g_1}{\sqrt{D}}\right)\frac{A}{C_s} \quad (1)$$

where A is the net assimilation rate (μmol m^{-2} s^{-1}), C_s (μmol mol^{-1}) and D (kPa) are the CO_2 concentration and the vapour pressure deficit at the leaf surface, respectively, and g_0 (mol m^{-2} s^{-1}), and g_1 are fitted constants representing the residual stomatal conductance when A reaches zero, and the slope of the sensitivity of g_s to A, respectively. The model was parameterised for different PFTs using data from Lin et al. (2015) (see De Kauwe et al. 2015).

In the standard version of CABLE, drought stress is implemented as an empirical scalar (β) that depends on soil moisture content, weighted by the fraction of roots in each of CABLE's six soil layers:

$$\beta = \sum_{i=1}^{n} f_{root,i} \frac{\theta_i - \theta_w}{\theta_{fc} - \theta_w};\ \beta \in [0,1] \quad (2)$$

where θ_i is the volumetric soil moisture content ($m^3\ m^{-3}$) in soil layer i, θ_w is the wilting point ($m^3\ m^{-3}$), θ_{fc} is the field capacity ($m^3\ m^{-3}$) and $f_{root,i}$ is the fraction of root mass in soil layer i. The six soil layers in CABLE have depths 0.022 m, 0.058 m, 0.154 m, 0.409 m, 1.085 m and 2.872 m. The factor β is assumed to limit the slope of the relationship between stomatal conductance (g_s, mol $m^{-2}\ s^{-1}$; Leuning 1995) by acting as a modifier on the parameter g_1.

In this study, we introduced a new expression for drought sensitivity of gas exchange, based on the work of Zhou et al. (2013, 2014). In this model, both g_1 and the photosynthetic parameters V_{cmax} and J_{max} are assumed to be sensitive to pre-dawn leaf water potential, but this sensitivity varies across species. There is considerable evidence that both g1 and V_{cmax} are sensitive to soil moisture (Keenan et al. 2009; Egea et al. 2011; Flexas et al. 2012; Zhou et al. 2013). There is also widespread evidence that plants are more directly respond to water potential rather than water content (Comstock and Mencuccini 1998; Verhoef and Egea, 2014).

Zhou et al. (2013) extended the optimal stomatal model of Medlyn et al. (2011) by fitting an exponential function to relate g_1 to pre-dawn leaf water potential (Ψ_{pd}):

$$g_1 = g_{1wet} \times \exp(b\Psi_{pd}) \quad (3)$$

where g_{1wet} is fitted parameter representing plant water use under well watered conditions (i.e. when $\Psi_{pd} = 0$) and b is a fitted parameter representing the sensitivity of g_1 to Ψ_{pd}. Species with different water use strategies can by hypothesised to differ in not only their g_1 parameter under well-watered conditions, g_{1wet} (see Lin et al. 2015), but also with the sensitivity to Ψ_{pd}, b. Zhou et al. (2013) also advanced a non-stomatal limitation to the photosynthetic biochemistry, which describes the apparent effect of water stress on V_{cmax}:

$$V_{cmax} = V_{cmax,wet} \frac{1 + \exp(S_f \Psi_f)}{1 + \exp(S_f (\Psi_f - \Psi_{pd}))} \quad (4)$$

where $V_{cmax,wet}$ is the V_{cmax} value in well watered conditions, S_f is a sensitivity parameter describing the steepness of the decline with water stress, Ψ_f is the water potential at which Ψ_{pd} decreases to half of its maximum value. As with g_1, it is hypothesised that in the same way species vary in their V_{cmax} values in well-watered conditions ($V_{cmax,wet}$), they would also differ in their sensitivity of down-regulated V_{cmax} with water stress (Zhou et al. 2014). In CABLE, as there is a constant ratio between the parameters J_{max} and V_{cmax}, the parameter J_{max} is similarly reduced by drought.

To implement Eq. (6) in CABLE we first had to convert soil moisture content (θ) to pre-dawn leaf water potential (Ψ_{pd}). We did so by assuming that overnight Ψ_{pd} and Ψ_S equilibrate before sunrise, thus ignoring any night-time transpiration (Dawson et al. 2007). Following Campbell (1974), we related θ to Ψ_S in each soil layer by:

$$\Psi_{S,i} = \Psi_e \left(\frac{\theta_i}{\theta_{sat}}\right)^{-k} \quad (5)$$

where Ψ_e is the air entry water potential (MPa) and k (unitless) is an empirical coefficient which is related to the soil texture. Values for Ψ_e and b are taken from CABLE's standard lookup table following Clapp and Hornberger (1978). We then needed to obtain a representative weighted estimate of Ψ_S across CABLE's soil layers. We tested three potential approaches for weighting in this paper:

(i) Using the root-biomass weighted θ and converting this to Ψ_S using Eq. (8), hereafter denoted M1. Such an approach is often favoured by models, following experimental evidence that plants preferentially access regions in the root zone where water is most freely available (Green and Clotheir 1995; Huang et al. 1997).

(ii) Taking the integrated θ over the top 5 soil layers (1.7 m depth) and converting this to Ψ_S using Eq. (8), hereafter denoted M2. This method assumes the plant effectively has access to an entire "bucket" of soil water. This approach is often favoured by "simpler" forest productivity models (e.g. Landsberg and Waring, 1997).

(iii) Weighting the average Ψ_S for each of the six soil layers by the weighted soil-to-root conductance to water uptake of each layer, following Williams et al. (1996; 2001), hereafter denoted M3. The total conductance term depends the combination of a soil component (R_s) and a root component (R_r). R_s is defined as (Gardner, 1960):

$$R_s = \frac{\ln\left(\frac{r_s}{r_r}\right)}{2\pi l_r D G_{soil}} \quad (6)$$

where r_s is the mean distance between roots (m), r_r is the fine root radius (m), D is the depth of the soil layer, G_{soil} is the soil conductivity (mmol m^{-1} s^{-1} MPa^{-1}) which depends on soil texture and soil water content, l_r is the fine root density (mm^{-3}). R_r is defined as:

$$R_r = \frac{R_r^*}{FD} \quad (7)$$

where R_r^* is the root resistivity (MPa s g $mmol^{-1}$), F is the root biomass per unit volume (g m^{-3}). This method weights Ψ_S to the upper soil layers when the soil is wet, but shifts towards layer lowers as the soil dries, due to the lower soil hydraulic conductance (e.g. Duursma et al. 2011).

2.3 Model simulations

During 2003, Europe experienced an anomalously dry summer, amplified by a combination of a preceding dry spring and high summer temperatures (Ciais et al. 2005; Schär et al. 2005). Summer temperatures were recorded to have exceeded the 30-year June-July-August (JJA) average by 3°C (Schär et al. 2005). Consequently we choose to focus our model comparisons on this period, in particular the period between June and September 2003.

At each of the five Fluxnet sites we ran three sets of simulations:

- A control simulation ("CTRL"), representing CABLE version 2.0.1.
- Three simulations to explore the new drought model using a "high" (*Quercus robur*), "medium" (*Quercus ilex*) and "low" (*Cedrus atlantica*) sensitivity to soil moisture.

Parameter values were obtained from the meta-analysis by Zhou et al. (2013; 2014) and are given in Table 1. For each of these simulations we also tested the three different methods of obtaining Ψ_S as described above.

- A "no drought" simulation in which any transpired water was returned to the soil. By comparing this simulation with either the control or any of the new drought model simulations (high, medium, low), a guide to the magnitude of the drought should be apparent.

Model parameters were not calibrated to match site characteristics; instead default PFT parameters were used for each site. Although CABLE has the ability to simulate full carbon, nitrogen and phosphorus biogeochemical cycling, this feature was not activated for this study, instead only the carbon and water cycle were simulated. For all simulations, leaf area index (LAI) was prescribed using CABLE's gridded monthly LAI climatology derived from Moderate-resolution Imaging Spectroradiometer (MODIS) LAI data (Knyazikhin et al. 1998; 1999) and the g_s scheme following Medlyn et al. (2011; see De Kauwe et al. 2015) was used throughout. All model simulations were spun-up by repeating the meteorological forcing site data until soil moisture and soil temperatures reached equilibrium (as we were ignoring the full biogeochemical cycling in these simulations).

2.4 Datasets used

To assess the performance of the CABLE model both with and without the new drought scheme, we selected a gradient of five forested Fluxnet (http://www.fluxdata.org/) sites across Europe (Table 2) from those available through the Protocol for the Analysis of Land Surface models (PALS; pals.unsw.edu.au; Abramowitz, 2012). These data have previously been pre-processed and quality controlled for use within the LSM community. Consequently, all site-years had near complete observations of key meteorological drivers (as opposed to significant gap-filled periods).

Model simulations were compared to measured latent heat and flux-derived gross primary productivity (GPP) at each of the FLUXNET sites. Flux-derived GPP estimates are calculated

from the measured net ecosystem exchange (NEE) of carbon between the atmosphere and the vegetation/soil, and the modelled ecosystem respiration (R_{eco}), where GPP is calculated as NEE + R_{eco}.

3 Results

Severity of the 2003 drought

Table 3 summarises summer differences in rainfall, air temperature, GPP and LE between 2002 and 2003 across the five sites covering the latitudinal gradient from mesic to xeric sites across Europe. Whilst the impact of the 2003 heatwave varied between sites, every site was warmer and drier in 2003. Similarly, GPP was lower at every site except Espirra, and LE was lower at three of the sites (Hesse, Roccarespampani and Castelporziano) in 2003 than in 2002.

Simulated fluxes during drought from the standard model

Figure 1 shows a site-scale comparison between standard CABLE (CTRL) transpiration (E), flux derived GPP, and the observed LE at the five sites. Table 4 and 5 shows a series of summary statistics (Root Mean Squared Error (RMSE), Nash-Sutcliffe efficiency (NSE), Pearsons's correlation coefficient (r) between modelled and observed GPP and LE. An indication of the severity of the drought can be obtained by comparing the difference between the "No drought" and the CTRL simulation.

For the two more mesic sites (Tharandt and Hesse), the CTRL simulation generally matched the trajectory of the observed LE, but displayed systematic periods of over-estimation (i.e. under-estimated the drought effect). By contrast, in the three more xeric sites (Roccarespampani, Castelporziano and Espirra), the reverse was true: the CTRL simulations descended into drought stress much more quickly than the observed fluxes. This rapid drought progression was particularly evident around day of year 155 at the Roccarespampani site. Across all sites, agreement with observed LE fluxes was generally poor (RMSE = 21.25 W m^{-2} to 38 W m^{-2}; NSE = –8.95 to 0.15). This outcome is partly a result of the high soil evaporation around mid-spring, which results in CABLE simulating very large LE fluxes during this period.

At Tharandt, Hesse and Roccarespampani, simulated GPP systematically underestimated the flux-derived peak GPP, particularly evident before day of year 180. Transitioning to the more xeric sites (Roccarespampani, Castelporziano and Espirra), simulated GPP was apparently too

sensitive to water stress, contributing to a poor agreement with flux-derived data (RMSE = 2.22 g C m^{-2} to 3.03 g C m^{-2}; NSE = –2.67 to 0.42).

Theoretical behaviour of new drought scheme

We now consider the implementation of the new drought model and the three sensitivity parameterisations. Figure 2a shows how leaf-level photosynthesis is predicted to decline (using Eqs. 3 and 4) in the new drought model with increasing water stress (more negative Ψ_S). The different sensitivities to drought are clearly visible, with the three parameterisations representing a spectrum of behaviour ranging from high to low drought sensitivity. Figures 2b and c show how the new drought model compares to the standard CABLE (CTRL; using Eq. 2) model on a sandy and clay soil type. The CTRL model is seen to most closely match the high sensitivity simulation on a sandy soil, but it predicts an earlier descent into drought stress. By contrast on the clay soil, the new medium and high sensitivity simulations encompass the predictions from the CTRL model. The new drought model and parameterisations afford a more flexible sensitivity to the down-regulation of photosynthesis with drought, which is particularly evident in the low sensitivity simulation.

Impact of new drought scheme on modelled LE

Figures 3–7 show the same site comparisons as Fig. 1, but with the addition of the new drought model and the three different ways (M1-3) in which Ψ_S can be averaged over the soil profile. Across all sites it is clear that using M1, the new drought model behaves in much the same way as the CTRL simulation. The explanation is that weighting Ψ_S by the fraction of roots in each layer, results in water being principally extracted from the top three shallow layers (Supplementary figures S1–S5). Consequently, small changes in θ result in a rapid decline in Ψ_S (owing to the non-linear relationship between θ and Ψ_S, Fig. 1), which causes an unrealistically abrupt shutdown of transpiration. M2 showed a greater separation between the three sensitivity parameterisations than method one. The greater separation is most evident at the xeric sites; the model performs particularly well at Espirra (LE RMSE < 16 W m^{-2} vs. CTRL RMSE = 35.31 W m^{-2}) and to a lesser extent at Castelporziano (LE low sensitivity RMSE = 19.72 W m^{-2} vs. CTRL RMSE = 31.76 W m^{-2}). Nevertheless, at the two mesic sites, the model completely underestimates the size of the drought, as a result of using a

large soil water bucket (1.7 m) to calculate Ψ_S. M3 in combination with the new drought model generally performed the best across all the sites, as it allows CABLE to simulate a more gradual reduction of fluxes during drought. At Roccarespampani a medium drought sensitivity performed best at reproducing the observed LE (CTRL RMSE = 38.0 W m^{-2} vs. 18.27 W m^{-2}), whilst at Espirra (CTRL RMSE = 35.31 W m^{-2} vs. 15.40 W m^{-2}) the low sensitivity performed best. At Castelporziano, both low (CTRL RMSE = 31.76 W m^{-2} vs. 20.41 W m^{-2}) and medium sensitivity (LE RMSE = 20.47 W m^{-2}) performed well. In contrast, at the two mesic sites, a high drought sensitivity performed best, although at both Hesse (LE CTRL RMSE = 21.25 W m^{-2} vs. 25.90 W m^{-2}) and Tharandt (LE CTRL RMSE = 28.5 W m^{-2} vs. 28.82 W m^{-2}), the new drought model performed marginally worse than the CTRL.

Impact of new drought scheme on modelled GPP

At the more xeric sites, there were noticeable improvements in simulated GPP during the drought period. Similar to the LE result, across all sites M3 worked best: using a medium drought sensitivity at both Roccarespampani (CTRL RMSE = 2.49 g C m^{-2} d^{-1} vs. 1.73 g C m^{-2} d^{-1}) and Castelporziano (CTRL RMSE = 2.22 g C m^{-2} d^{-1} vs. 0.95 g C m^{-2} d^{-1}), and a low sensitivity at Espirra (CTRL RMSE = 3.03 g C m^{-2} d^{-1} vs. 1.43 g C m^{-2} d^{-1}). At the mesic end of the gradient, a medium sensitivity at Hesse (CTRL RMSE = 2.85 g C m^{-2} d^{-1} vs. 2.71 g C m^{-2} d^{-1}) and a medium or high sensitivity at Tharandt worked best; although using either sensitivity performed slightly worse than the CTRL (CTRL RMSE = 2.06 g C m^{-2} d^{-1} vs. >= 2.23 g C m^{-2} d^{-1}).

4 Discussion

Experimental data suggest that plants exhibit a continuum of drought sensitivities, with species originating in more mesic environments showing higher sensitivity than species from more xeric environments (Bahari et al. 1985; Reich and Hinckley, 1989; Ni and Pallardy, 1991; Zhou et al. 2014). We investigated whether variable drought sensitivity improves the ability of the CABLE LSM to reproduce observed drought impacts across a latitudinal gradient. We found that, at the mesic sites, a high drought sensitivity was required; moving southwards towards more xeric sites, the sensitivity parameterisation transitioned to a medium and finally to a low drought sensitivity. This work demonstrates the importance of understanding how plant traits vary with climate across the landscape. However, our analysis also highlighted the importance of identifying which soil layers matter most to the plant: our results depended strongly on how we weighted soil moisture availability through the profile.

Weighting soil moisture availability

Commonly, empirical dependences of gas exchange on soil moisture content or potential (Eqns 3, 4) are estimated from pot experiments (e.g. Zhou et al. 2013; 2014), in which it is fair to assume that the soil moisture content is relatively uniform and fully explored by roots. In contrast, soil moisture content and rooting depth in the field typically have strong vertical profiles. Thus, to implement such equations in a land surface model requires that we specify how to weight the soil layers to obtain a representative value of whole-profile θ or Ψ_S. In this study we tested three potential implementations. Our first approach was to weight each layer by root biomass. Evidence suggests that plants preferentially access regions in the root zone where water is most freely available (Green and Clotheir 1995; Huang et al. 1997). Hence, many models follow this approach: for example, the original version of CABLE weighted soil moisture content by root biomass (Eqn 2) while the Community Land Model (CLM) estimates a water stress factor based on a root-weighted Ψ_S, using a PFT-defined minimum and maximum water potential (Oleson et al. 2013). However, we found that this approach performed poorly. We observed an 'on-off' behaviour in response to drought, which occurs because the behaviour of the model is driven by the top soil layers, whose total soil moisture content is relatively small and root biomass is relatively high, and can be depleted rapidly, leading to a sudden onset of severe drought. Many other LSMs show this abrupt effect of

415 drought (Egea et al., 2011; Powell et al., 2013). Powell et al. (2013) found that four models
416 (CLM version 3.5, Integrated BIosphere Simulator version 2.6.4 (IBIS), Joint UK Land
417 Environment Simulator version 2.1 (JULES), and Simple Biosphere model version 3 (SiB3))
418 implement abrupt transitions of this kind. We also found that with this weighting of soil
419 layers, there was little effect of variable drought sensitivity: the depletion of soil moisture
420 content of the top layers is so rapid that there is little difference between low and high
421 sensitivities to drought. Such an outcome suggests that there is little adaptive significance of
422 drought sensitivity, which seems unlikely. A further implication of using a root-weighted
423 function to calculate Ψ_S is that two distinctly different scenarios, a soil that has been very wet
424 but experienced a short dry period, allowing the topsoil to dry, and a soil that has had a
425 prolonged period of drought but experienced a recent rainfall event, would have similar
426 impacts on gas exchange. Again, this outcome seems unlikely.

427

428 We tested a second implementation in which soil moisture potential was calculated from the
429 moisture content of the entire rooting zone (top five soil layers = 1.7 m). Such an approach is
430 commonly used in forest productivity models (e.g. Landsberg and Waring, 1997). However,
431 this approach severely underestimates drought impacts because the moisture content of the
432 total soil profile is so large, meaning that it is rarely depleted enough to impact on gas
433 exchange.

434

435 In reality, plant water uptake shifts lower in the profile as soil dries out (e.g. Duursma et al.
436 2011). Thus, in our third implementation, we tested an approach in which the weighting of
437 soil layers moves downwards as drought progresses. This approach is effectively similar to
438 that used by the soil–plant–atmosphere (SPA) model (Williams et al. 1996; 2001), in which
439 soil layers are weighted by their soil-to-root conductance, which declines as the moisture
440 content declines. Of the three approaches we tested, this method performed best, allowing
441 CABLE to replicate the observations across the latitudinal mesic to xeric gradient. This
442 dynamic weighting of Ψ_S may partially explain previous good performance by SPA in other
443 model inter-comparisons focussed on drought (e.g. Powell et al. 2013). Recently, Bonan et al.
444 (2014) tested the suitability of using a model that considers optimal stomatal behaviour and
445 plant hydraulics (SPA; Williams et al. 1996) for earth system modelling, and demonstrated

446 marked improvement over the standard model during periods of drought stress. We thus
447 suggest that models using a soil moisture stress function to simulate drought effects on gas
448 exchange should consider a dynamic approach to weighting the contribution of different soil
449 layers.

450

451 We note that this issue is related to another long-standing problem for LSMs: that of
452 determining the vertical distribution of root water uptake (e.g. Feddes et al., 2001; Federer et
453 al., 2003; Kleidon and Heimann, 1998, 2000). In the standard version of CABLE, water
454 uptake from each soil layer initially depends on the fraction of root biomass in each layer, but
455 moves downwards during drought as the upper layers are depleted. It is possible that changes
456 to the weighting of soil moisture in determining drought sensitivity should also be
457 accompanied by changes to the distribution of root water uptake, but we did not explore this
458 option here. Li et al. (2012) previously tested an alternative dynamic root water uptake
459 function (Lai and Katul, 2000) in CABLE, but found little improvement in predicted LE
460 during seasonal droughts without also considering a mechanism for hydraulic redistribution.
461 Further work should evaluate models not only against LE fluxes, but also against
462 measurements of soil moisture profiles. Many experimental sites now routinely install
463 multiple soil moisture sensors (e.g. direct gravimetric sampling, neutron probes, time domain
464 reflectometry), which provide accurate insight into root water extraction and hydraulic
465 redistribution, even down to considerable depths (>4 m). These data have thus far been
466 underutilised for model improvement, but should be a priority for reducing the uncertainty in
467 soil moisture dynamics.

468

469 *Incorporating different sensitivities to drought*

470 Using the third and best method to calculate overall Ψ_s, we found that varying drought
471 sensitivity across sites enabled the model to better capture drought effects across the
472 mesic/xeric gradient, with a high drought sensitivity implied in mesic sites and a low drought
473 sensitivity implied in xeric sites. These results should not be surprising, given the increasing
474 amount of experimental evidence suggesting that drought sensitivity varies among species
475 and across climates (e.g. Engelbrecht and Kursar, 2003; Engelbrecht et al. 2007; Skelton et al.
476 2015). In contrast to these data, most LSMs assume a single parameterisation for drought

sensitivity, which is typically based on mesic vegetation. Our results suggest that such a parameterisation is very likely to overstate the impacts of drought on both carbon and water fluxes in drier regions.

Our work thus underlines a need to move beyond models that implement drought sensitivity through a single PFT parameterisation. In order to capture the observed variability in plant responses to drought, models need to consider a continuum of sensitivities. It is, of course, challenging to implement such a continuum in a global vegetation model. In this study, we used a simple site-specific approach in which we selected three sets of model parameters from a meta-analysis by Zhou et al. (2013; 2014), allowing us to characterise a range of plant responses to drought. Global vegetation models would require a more sophisticated approach that relates drought sensitivity to the climate of each pixel. One potential solution would be to develop an empirical correlation between drought sensitivity and a long-term moisture index (e.g. the ratio of mean precipitation to the equilibrium evapotranspiration; Cramer and Prentice, 1988; Gallego-Sala et al. 2010). Previous studies have demonstrated the feasibility of linking model parameters that determine plant water use strategy to such a moisture index in global simulations (Wang et al. 2014; De Kauwe et al. 2015). Such an approach would requires a concerted effort to collate appropriate data, as there are few compilations to date of traits related to drought sensitivity (but see Manzoni et al. 2011; Zhou et al. 2013). Another, more challenging, alternative, would be to develop optimization hypotheses that can predict vegetation drought sensitivity from climate (e.g. Manzoni et al. 2014).

Further model uncertainties

Whilst this work advances the ability of LSMs to simulate drought, it does not address all processes needed to correctly capture drought impacts. Other issues to consider include: (i) rooting depth; (ii) leaf shedding; (iii) soil evaporation; and (iv) soil heterogeneity, among others.

Here we have assumed that all sites had the soil depth (4.6 m), with rooting depth distributed exponential through the profile, as is commonly used in LSMs. However, this assumption may be incorrect. Access to water by deep roots could be a potential alternative explanation

for the low drought sensitivity that we inferred at the southernmost (xeric) site, Espirra. Here the dominant species is not native to the region, but rather a plantation of blue gum (*Eucalyptus globulus*), a species that is generally found to have high, not low, drought sensitivity (White 1996; Mitchell et al. 2014). Many eucalypts have a deep rooting strategy (Fabiao et al. 1987), suggesting a possible alternative explanation for drought tolerance at this site. More in-depth study of fluxes and soil moisture patterns at this site would be needed to determine the role of rooting depth.

During droughts, plants are often observed to shed their leaves. This is a self-regulatory mechanism to reduce water losses (Tyree et al. 1993; Jonasson et al. 1997; Bréda et al. 2006). During the 2003 heatwave at Hesse, an early reduction of approximately 1.7 m^2 m^{-2} was observed. Similarly, at Brasschaat there was a observed reduction of 0.8 m^2 m^{-2} and at Tharandt needle-litter was increased during September until November, with LAI estimated to be 0.9 m^2 m^{-2} lower (Bréda et al. 2006; Granier et al. 2007). In contrast, models typically fix turnover rates for leaves and as such this feedback is largely absent from models. During periods of water stress, models do simulate an indirect reduction in LAI via down-regulated net primary productivity, but this feedback is much slower than is commonly observed. Not accounting for this canopy-scale feedback will result in models over-estimating carbon and water fluxes and thus losses in θ during drought.

Existing models also disagree as to the mechanism by which to down-regulate productivity during periods of water stress (De Kauwe et al. 2013). In the standard version of CABLE, only the slope of the relationship between g_s and A is reduced by water stress. The SPA model behaves similarly. In contrast, JULES (Clark et al. 2011) and the Sheffield Dynamic Global Vegetation Model (SDGVM; Woodward and Lomas, 2004), down-regulate the photosynthetic capacity via the biochemical parameters V_{cmax} and J_{max} (maximum electron transport rate). Here, we assumed that water stress affects both the slope of g_s-A and the biochemical parameters V_{cmax} and J_{max}, supported by results from Zhou et al. (2013, 2014). We did not evaluate this assumption against the eddy flux data. However, previous studies have also suggested that both effects are needed to explain responses of fluxes during drought (Keenan et al. 2010).

539

540 Finally, although models do have the capacity to simulate vertical variations in θ, they do not
541 always represent horizontal sub-grid scale variability. This assumption is likely to contribute
542 to the abruptness of modelled transitions from well-watered to completely down-regulated
543 carbon and water fluxes. Earlier work by Entekhabi and Eagleson (1989), and models such as
544 the variable infiltration capacity (VIC) model (Liang et al. 1994), and most recently Decker
545 2015 (submitted) have attempted to address this issue by employing statistical distributions to
546 approximate horizontal spatial heterogeneity in soil moisture (see also Crow and Wood,
547 2002). These parsimonious approaches typically require few parameters, making them
548 attractive in the LSM context and potentially suitable for modelling ecosystem and
549 hydrological responses to drought (Luo et al. 2013).

550

551 *Testing models against extreme events*

552 In conclusion, we have used a model evaluation against flux measurements during a large-
553 scale heatwave event to make significant progress in modelling of drought impacts. While
554 model evaluation against data is now commonplace (Prentice et al. 2015) and has recently
555 been extended to formal benchmarking, particularly in the land surface community
556 (Abramowitz, 2005; Best et al. 2015), many of these benchmarking indicators are based on
557 seasonal or annual outputs and thus miss the opportunity to examine model performance
558 during extreme events. Model projections under future climate change require good
559 mechanistic representations of the impacts of extreme events. However, responses to extreme
560 events are rarely evaluated and there is therefore an urgent need to orient model testing to
561 periods of extremes. To that end, precipitation manipulation experiments (e.g. Nepstad et al.
562 2002; Hanson et al. 2003; Pangle et al. 2012) represent a good example of a currently under-
563 exploited avenue (but see Fisher et al. 2007; Powell et al. 2013) that could be used for model
564 evaluation and/or benchmarking (Smith et al. 2014). However, we urge that these exercises do
565 not focus solely on overall model performance, but also test the realism of individual model
566 assumptions (Medlyn et al. 2015).

567

568

569

Acknowledgements

This work was supported by the Australian Research Council (ARC) Linkage grant LP140100232 and the ARC Centre of Excellence for Climate System Science (CE110001028). SZ was supported by an international Macquarie University Research Excellence Scholarship. This work is also a contribution to the AXA Chair Programme in Biosphere and Climate Impacts and the Imperial College initiative on Grand Challenges in Ecosystems and the Environment. We thank CSIRO and the Bureau of Meteorology through the Centre for Australian Weather and Climate Research for their support in the use of the CABLE model. This work used eddy covariance data acquired by the FLUXNET community for the La Thuile FLUXNET release, supported by the following networks: AmeriFlux (U.S. Department of Energy, Biological and Environmental Research, Terrestrial Carbon Program (DE-FG02-04ER63917 and DE-FG02-04ER63911)), AfriFlux, AsiaFlux, CarboAfrica, CarboEuropeIP, CarboItaly, CarboMont, ChinaFlux, Fluxnet-Canada (supported by CFCAS, NSERC, BIOCAP, Environment Canada, and NRCan), GreenGrass, KoFlux, LBA, NECC, OzFlux, TCOS-Siberia, USCCC. We acknowledge the financial support to the eddy covariance data harmonization provided by CarboEuropeIP, FAO-GTOS-TCO, iLEAPS, Max Planck Institute for Biogeochemistry, National Science Foundation, University of Tuscia, Université Laval and Environment Canada and US Department of Energy and the database development and technical support from Berkeley Water Center, Lawrence Berkeley National Laboratory, Microsoft Research eScience, Oak Ridge National Laboratory, University of California - Berkeley, University of Virginia. All data analysis and plots were generated using the Python language and the Matplotlib plotting library (Hunter, 2007).

References

Abramowitz, G.: Towards a benchmark for land surface models, Geophys. Res. Lett., 32, L22702, 2005.

Abramowitz, G.: Towards a public, standardized, diagnostic benchmarking system for land surface models, Geosci. Model Dev., 5, 819–827, 2012.

Abramowitz, G., Leuning, R., Clark, M. and Pitman, A.: Evaluating the Performance of Land Surface Models, J. Clim., 21, 5468–5481, 2008.

Allen, C. D., Macalady, A. K., Chenchouni, H., Bachelet, D., McDowell, N., Vennetier, M., Kitzberger, T., Rigling, A., Breshears, D. D., Hogg, E. H. (Ted), Gonzalez, P., Fensham, R., Zhang, Z., Castro, J., Demidova, N., Lim, J.-H., Allard, G., Running, S. W., Semerci, A. and Cobb, N.: A global overview of drought and heat-induced tree mortality reveals emerging climate change risks for forests, For. Ecol. Manag., 259, 660–684, 2010.

Anderegg, W. R., Kane, J. M. and Anderegg, L. D.: Consequences of widespread tree mortality triggered by drought and temperature stress, Nat. Clim. Change, 3, 30–36, 2013.

Bahari, Z. A., Pallardy, S. G. and Parker, W.C. Photosynthesis, water relations, and drought adaptation in six woody species of oak-hickory forests in central Missouri. For. Sci. 31:557-569, 1985.

Best, M. J., Abramowitz, G., Johnson, H. R., Pitman, A. J., Balsamo, G. and Boone, A., Cuntz, M., Decharme, B., Dirmeyer, P. A., Dong, J., Ek, M., Guo, Z., Haverd, V., van den Hurk, B. J. J., Nearing, G. S., Pak, B., Peters-Lidard, C., Santanello Jr., J. A., Stevens, L. and Vuichard, N.: The Plumbing of Land Surface Models: Benchmarking Model Performance. J. Hydrometeor, 16, 1425–1442, 2015.

629 Bonan, G., Williams, M., Fisher, R. and Oleson, K.: Modeling stomatal conductance in the
630 Earth system: linking leaf water-use efficiency and water transport along the soil-plant-
631 atmosphere continuum, Geosci. Model Dev., 7, 2193–2222, 2014.

632

633 Bréda, N., Huc, R., Granier, A. and Dreyer, E.: Temperate forest trees and stands under severe
634 drought: a review of ecophysiological responses, adaptation processes and long-term
635 consequences, Ann. For. Sci., 63, 625–644, 2006.

636

637 Breshears, D. D., Cobb, N. S., Rich, P. M., Price, K. P., Allen, C. D., Balice, R. G., Romme,
638 W. H., Kastens, J. H., Floyd, M. L., Belnap, J., Anderson, J. J., Myers, O. B. and Meyer, C.
639 W.: Regional vegetation die-off in response to global-change-type drought, Proc. Natl. Acad.
640 Sci. U. S. A., 102, 15144–15148, 2005.

641

642 Campbell, G. S.: A simple method for determining unsaturated conductivity from moisture
643 retention data., Soil Sci., 117, 311–314, 1974.

644

645 Canadell, J., Jackson, R., Ehleringer, J., Mooney, H., Sala, O. and Schulze, E.-D.: Maximum
646 rooting depth of vegetation types at the global scale, Oecologia, 108, 583–595, 1996.

647

648 Chaves, M. M., Maroco, J. P. and Pereira, J. S.: Understanding plant responses to drought—
649 from genes to the whole plant, Funct. Plant Biol., 30, 239–264, 2003.

650

651 Choat, B., Jansen, S., Brodribb, T. J., Cochard, H., Delzon, S., Bhaskar, R., Bucci, S. J., Feild,
652 T. S., Gleason, S. M., Hacke, U. G., Jacobsen, A. L., Lens, F., Maherali, H., Martinez-Vilalta,
653 J., Mayr, S., Mencuccini, M., Mitchell, P. J., Nardini, A., Pittermann, J., Pratt, R. B., Sperry,
654 J. S., Westoby, M., Wright, I. J. and Zanne, A. E.: Global convergence in the vulnerability of
655 forests to drought, Nature, 491, 752–755, 2012.

656

657 Ciais, P., Reichstein, M., Viovy, N., Granier, A., Ogee, J., Allard, V., Aubinet, M.,
658 Buchmann, N., Bernhofer, C., Carrara, A., Chevallier, F., De Noblet, N., Friend, A. D.,
659 Friedlingstein, P., Grunwald, T., Heinesch, B., Keronen, P., Knohl, A., Krinner, G., Loustau,

660 D., Manca, G., Matteucci, G., Miglietta, F., Ourcival, J. M., Papale, D., Pilegaard, K.,
661 Rambal, S., Seufert, G., Soussana, J. F., Sanz, M. J., Schulze, E. D., Vesala, T. and Valentini,
662 R.: Europe-wide reduction in primary productivity caused by the heat and drought in 2003,
663 Nature, 437, 529–533, 2005.

664

665 Clapp, R. B. and Hornberger, G. M.: Empirical equations for some soil hydraulic properties,
666 Water Resour. Res., 14, 601–604, 1978.

667

668 Clark, D. B., Mercado, L. M., Sitch, S., Jones, C. D., Gedney, N., Best, M. J., Pryor, M.,
669 Rooney, G. G., Essery, R. L. H., Blyth, E., Boucher, O., Harding, R. J., Huntingford, C. and
670 Cox, P. M.: The Joint UK Land Environment Simulator (JULES), model description - Part 2:
671 Carbon fluxes and vegetation dynamics, Geosci. Model Dev., 4, 701–722, 2011.

672

673 Comstock, J. and Mencuccini, M.: Control of stomatal conductance by leaf water potential in
674 Hymenoclea salsola (T. & G.), a desert subshrub, Plant Cell Environ., 21, 1029–1038, 1998.

675

676 Cowan, I. and Farquhar, G.: Stomatal function in relation to leaf metabolism and
677 environment., in Society for Experimental Biology Symposium, Integration of Activity in the
678 Higher Plant, vol. 31, edited by D. H. Jennings, pp. 471–505, Cambridge University Press.,
679 1977.

680

681 Cramer, W. and Prentice, I.: Simulation of regional soil moisture deficits on a European scale,
682 Nor. Geogr. Tidsskr. - Nor. J. Geogr., 42, 149–151, 1988.

683

684 Crow, W. T and Wood, E. F.: Impact of soil moisture aggregation on surface energy flux
685 prediction during SGP'97. Geophys. Res. Lett., 29. 8-1, 2002.

686

687 Cruz, F. T., Pitman, A. J. and Wang, Y.-P.: Can the stomatal response to higher atmospheric
688 carbon dioxide explain the unusual temperatures during the 2002 Murray-Darling Basin
689 drought?, J. Geophys. Res. Atmospheres, 115(D2), 2010.

690
691 Dai, A.: Increasing drought under global warming in observations and models, Nat. Clim.
692 Change, 3, 52–58, 2013.
693
694 Dawson, T. E., Burgess, S. S., Tu, K. P., Oliveira, R. S., Santiago, L. S., Fisher, J. B.,
695 Simonin, K. A. and Ambrose, A. R.: Nighttime transpiration in woody plants from contrasting
696 ecosystems, Tree Physiol., 27, 561–575, 2007.
697
698 Decker, M., A new Soil Moisture and Runoff Parameterization for the CABLE LSM
699 including subgrid scale processes, J. Adv. Model Earth Sy., submitted, 2015.
700
701 De Kauwe, M. G., Medlyn, B. E., Zaehle, S., Walker, A. P., Dietze, M. C., Hickler, T., Jain,
702 A. K., Luo, Y., Parton, W. J., Prentice, I. C., Smith, B., Thornton, P. E., Wang, S., Wang, Y.-
703 P., Waarlind, D., Weng, E., Crous, K. Y., Ellsworth, D. S., Hanson, P. J., Seok Kim, H.-,
704 Warren, J. M., Oren, R. and Norby, R. J.: Forest water use and water use efficiency at
705 elevated CO_2: a model-data intercomparison at two contrasting temperate forest FACE sites,
706 Glob. Change Biol., 19, 1759–1779, 2013.
707
708 De Kauwe, M. G., Kala, J., Lin, Y.-S., Pitman, A. J., Medlyn, B. E., Duursma, R. A.,
709 Abramowitz, G., Wang, Y.-P. and Miralles, D. G.: A test of an optimal stomatal conductance
710 scheme within the CABLE land surface model, Geosci. Model Dev., 8, 431–452, 2015.
711
712 Duursma, R., Kolari, P., Perämäki, M., Nikinmaa, E., Hari, P., Delzon, S., Loustau, D.,
713 Ilvesniemi, H., Pumpanen, J. and Mäkelä, A.: Predicting the decline in daily maximum
714 transpiration rate of two pine stands during drought based on constant minimum leaf water
715 potential and plant hydraulic conductance, Tree Physiol., 28, 265–276, 2008.
716
717 Duursma, R. A., Barton, C. V. M., Eamus, D., Medlyn, B. E., Ellsworth, D. S., Forster, M. A.,
718 Tissue, D. T., Linder S., McMurtrie, R. E. Rooting depth explains [CO_2] × drought interaction
719 in Eucalyptus saligna. Tree Physiol., 31, 922–931, 2011.
720

721 Egea, G., Verhoef, A. and Vidale, P. L.: Towards an improved and more flexible
722 representation of water stress in coupled photosynthesis–stomatal conductance models, Agric.
723 For. Meteorol., 151, 1370–1384, 2011.

724

725 Engelbrecht, B. M. J., Comita, L. S., Condit, R., Kursar, T. A., Tyree, M. T., Turner, B. L.,
726 Hubbell, S. P.: Drought sensitivity shapes species distribution patterns in tropical forests.
727 Nature, 447, 80-82.

728 Engelbrecht, B. M. J. and Kursar, T. A. Comparative drought-resistance of seedlings of 28
729 species of co-occurring tropical woody plants. Oecologia, 136, 383–393, 2003.

730

731 Entekhabi, D. and Eagleson, P. S.: Land surface hydrology parameterization for atmospheric
732 general circulation models including subgrid scale spatial variability, J. Clim., 2, 816–831,
733 1989.

734

735 Fabião A., Madeira M., Steen E.: Root mass in plantations of Eucalyptus globulus in Portugal
736 in relation to soil characteristics. Arid Soil Res. Rehabil 1, 185-194, 1987.

737

738 Feddes, R. A., Hoff, H., Bruen, M., Dawson, T., de Rosnay, P., Dirmeyer, P., Jackson, R. B.,
739 Kabat, P., Kleidon, A., Lilly, A. and Pitman, A. J.: Modeling root water uptake in
740 hydrological and climate models, Bull. Am. Meteorol. Soc., 82, 2797–2809, 2001.

741

742 Federer, C., Vörösmarty, C. and Fekete, B.: Sensitivity of annual evaporation to soil and root
743 properties in two models of contrasting complexity, J. Hydrometeorol., 4, 1276–1290, 2003.

744

745 Fensham, R., Fairfax, R. and Ward, D.: Drought-induced tree death in savanna, Glob. Change
746 Biol., 15, 380–387, 2009.

747

748 Fischer, E., Seneviratne, S., Lüthi, D. and Schär, C.: Contribution of land-atmosphere
749 coupling to recent European summer heat waves, Geophys. Res. Lett., 34, 2007.

Flexas, J., Barbour, M. M., Brendel, O., Cabrera, H. M., Carriquí, M., Díaz-Espejo, A., Douthe, C., Dreyer, E., Ferrio, J. P., Gago, J., Gallé, A., Galmés, J., Kodama, N., Medrano, H., Niinemets, Ü., Peguero-Pina, J. J., Pou, A., Ribas-Carbó, M., Tomás, M., Tosens, T. and Warren, C. R.: Mesophyll diffusion conductance to CO_2: an unappreciated central player in photosynthesis, Plant Sci., 193, 70–84, 2012.

Galbraith, D., Levy, P. E., Sitch, S., Huntingford, C., Cox, P., Williams, M. and Meir, P.: Multiple mechanisms of Amazonian forest biomass losses in three dynamic global vegetation models under climate change, New Phytol., 187, 647–665, 2010.

Gallego-Sala, A., Clark, J., House, J., Orr, H., Prentice, I. C., Smith, P., Farewell, T. and Chapman, S.: Bioclimatic envelope model of climate change impacts on blanket peatland distribution in Great Britain, Clim. Res., 45, 151–162, 2010.

Garcia-Forner, N., Adams, H. D., Sevanto, S., Collins, A. D., Dickman, L. T., Hudson, P. J., Zeppel, M., Martínez-Vilalta, J. and Mcdowell, N. G.: Responses of two semiarid conifer tree species to reduced precipitation and warming reveal new perspectives for stomatal regulation, Plant Cell Amp Environ., in press, 2015.

Gerten, D., Luo, Y., Le Maire, G., Parton, W. J., Keough, C., Weng, E., Beier, C., Ciais, P., Cramer, W., Dukes, J. S., Hanson, P. J., Knapp, A. A. K., Linder, S., Nepstad, D., Rustad, L. and Sowerby, A.: Modelled effects of precipitation on ecosystem carbon and water dynamics in different climatic zones, Glob. Change Biol., 14, 2365–2379, 2008.

Green, S. R. and Clothier, B. E.: Root water uptake by kiwifruit vines following partial wetting of the root zone. Plant Soil, 173, 317-328, 1995.

Hanson, P. J., M. A. Huston, and D. E. Todd: Walker branch throughfall displacement experiment, in North American Temperate Deciduous Forest Responses to Changing

780 Precipitation Regimes, edited by P. J. Hanson and S. D. Wullschleger, pp. 8–31, Springer,
781 New York, 2003.
782
783 Huang, B., R. R. Duncan, and R. N. Carrow (1997), Drought-resistance mechanisms of seven
784 warm-season turfgrasses under surface soil drying: II. Root aspects, Crop Sci., 37, 1863–
785 1869.
786
787 Hunter, J. D.: Matplotlib: A 2D graphics environment, Comput. Sci. Amp Eng., 9, 90–95,
788 2007.
789
790 Keenan, T., García, R., Friend, A., Zaehle, S., Gracia, C. and Sabate, S.: Improved
791 understanding of drought controls on seasonal variation in Mediterranean forest canopy CO_2
792 and water fluxes through combined in situ measurements and ecosystem modelling,
793 Biogeosciences, 6, 1423–1444, 2009.
794
795 Keenan, T., Sabate, S. and Gracia, C.: The importance of mesophyll conductance in
796 regulating forest ecosystem productivity during drought periods, Glob. Change Biol., 16,
797 1019–1034, 2010.
798
799 Kleidon, A. and Heimann, M.: A method of determining rooting depth from a terrestrial
800 biosphere model and its impacts on the global water and carbon cycle, Glob. Change Biol., 4,
801 275–286, 1998.
802
803 Klein, T.: The variability of stomatal sensitivity to leaf water potential across tree species
804 indicates a continuum between isohydric and anisohydric behaviours, Funct. Ecol., 28, 1313–
805 1320, 2014.
806
807 Knyazikhin, Y., Marshak, J. V., Diner, D. J., B, M. R., Verstraete, M., B, P. and Gobron, N.:
808 Estimation of vegetation canopy leaf area index and fraction of absorbed photosynthetically

809 active radiation from atmosphere-corrected MISR data, J. Geophys. Res., 103, 32239–32257,
810 1998.
811
812 Knyazikhin, Y., Glassy, J., Privette, J. L., Tian, Y., Lotsch, A., Zhang, Y., Wang, Y.,
813 Morisette, J. T., P.Votava, Myneni, R. B., Neman, R. R. and Running, S. W.: MODIS Leaf
814 Area Index (LAI) and Fraction of Photosynthetically Active Radiation Absorbed by
815 Vegetation (FPAR) Product (MOD15) Algorithm Theoretical Basis Document. [online]
816 Available from: http://eospso.gsfc.nasa.gov/atbd/modistables.html, 1999.
817
818 Kowalczyk, E., Stevens, L., Law, R., Dix, M., Wang, Y., Harman, I., Haynes, K., Srbinovsky,
819 J., Pak, B. and Ziehn, T.: The land surface model component of ACCESS: description and
820 impact on the simulated surface climatology, Aust Meteorol Ocean. J, 63, 65–82, 2013.
821
822 Kowalczyk, E. A., Wang, Y. P., Wang, P., Law, R. H. and Davies, H. L.: The CSIRO
823 Atmosphere Biosphere Land Exchange (CABLE) model for use in climate models and as an
824 offline model, CSIRO, 2006.
825
826 Lai, C. T. and Katul, G.: The dynamic role of root-water uptake in coupling potential to actual
827 transpiration, Adv. Water Resour., 23, 427–439, 2000.
828
829 Landsberg, J. and Waring, R.: A generalised model of forest productivity using simplified
830 concepts of radiation-use efficiency, carbon balance and partitioning, For. Ecol. Manag., 95,
831 209–228, 1997.
832
833 Leuning, R.: A critical appraisal of a combined stomatal-photosynthesis model for C_3 plants.,
834 Plant Cell Environ., 18, 339–355, 1995.
835
836 Lewis, S. L., Brando, P. M., Phillips, O. L., van der Heijden, G. M. and Nepstad, D.: The
837 2010 amazon drought, Science, 331, 554–554, 2011.
838

Li, L., Wang, Y.-P., Yu, Q, Pak, B., Eamus, D., Yan, J., van Gorsel, E. and Baker, I. T.: Improving the responses of the Australian community land surface model (CABLE) to seasonal drought. J. Geophys. Res-Biogeo., 117, G4, 2012.

Liang, X., Lettenmaier, D. P., Wood, E. F. and Burges, S. J.: A simple hydrologically based model of land surface water and energy fluxes for general circulation models, J. Geophys. Res.- Ser.-, 99, 14–415, 1994.

Limousin, J.-M., Bickford, C. P., Dickman, L. T., Pangle, R. E., Hudson, P. J., Boutz, A. L., Gehres, N., Osuna, J. L., Pockman, W. T. and McDowell, N. G.: Regulation and acclimation of leaf gas exchange in a piñon–juniper woodland exposed to three different precipitation regimes, Plant Cell Environ., 36, 1812–1825, 2013.

Lin, Y.-S., Medlyn, B. E., Duursma, R. A., Prentice, I. C., Wang, H., Baig, S., Eamus, D., de Dios, V. R., Mitchell, P., Ellsworth, D. S., de Beeck, M. O., Wallin, G., Uddling, J., Tarvainen, L., Linderson, M.-L., Cernusak, L. A., Nippert, J. B., Ocheltree, T. W., Tissue, D. T., Martin-StPaul, N. K., Rogers, A., Warren, J. M., De Angelis, P., Hikosaka, K., Han, Q., Onoda, Y., Gimeno, T. E., Barton, C. V. M., Bennie, J., Bonal, D., Bosc, A., Low, M., Macinins-Ng, C., Rey, A., Rowland, L., Setterfield, S. A., Tausz-Posch, S., Zaragoza-Castells, J., Broadmeadow, M. S. J., Drake, J. E., Freeman, M., Ghannoum, O., Hutley, L. B., Kelly, J. W., Kikuzawa, K., Kolari, P., Koyama, K., Limousin, J.-M., Meir, P., Lola da Costa, A. C., Mikkelsen, T. N., Salinas, N., Sun, W. and Wingate, L.: Optimal stomatal behaviour around the world, Nat. Clim. Change, 5, 459–464, 2015.

Lorenz, R., Pitman, A., Donat, M., Hirsch, A., Kala, J., Kowalczyk, E., Law, R. and Srbinovsky, J.: Representation of climate extreme indices in the ACCESS1. 3b coupled atmosphere-land surface model, Geosci. Model Dev., 7, 545–567, 2014.

Luo, X., Liang, X., and McCarthy, H. R.: VIC+ for water-limited conditions: a study of biological and hydrological processes and their interactions in the soil-plant-atmosphere continuum, Water Resour. Res., 49, 7711-7732, 2013.

Mahfouf, J.-F., Ciret, C., Ducharne, A., Irannejad, P., Noilhan, J., Shao, Y., Thornton, P., Xue, Y. and Yang, Z.-L.: Analysis of transpiration results from the RICE and PILPS workshop, Glob. Planet. Change, 13, 73–88, 1996.

Manzoni, S.: Integrating plant hydraulics and gas exchange along the drought-response trait spectrum. Tree Physiol, 34, 1031-1034, 2014.

Manzoni, S., Vico, G., Katul, G., Fay, P. A., Polley, W., Palmroth, S. and Porporato, A. Optimizing stomatal conductance for maximum carbon gain under water stress: a meta-analysis across plant functional types and climates. Funct. Ecol., 25, 456-467, 2011.

Mao, J., Pitman, A. J., Phipps, S. J., Abramowitz, G. and Wang, Y.: Global and regional coupled climate sensitivity to the parameterization of rainfall interception, Clim. Dyn., 37, 171–186, 2011.

McDowell, N., Pockman, W. T., Allen, C. D., Breshears, D. D., Cobb, N., Kolb, T., Plaut, J., Sperry, J., West, A., Williams, D. G. and others: Mechanisms of plant survival and mortality during drought: why do some plants survive while others succumb to drought?, New Phytol., 178, 719–739, 2008.

McDowell, N. G. and Allen, C. D.: Darcy's law predicts widespread forest mortality under climate warming, Nat. Clim. Change, 5, 669–672, 2015.

Medlyn, B. E. and Zaehle, S. and De Kauwe, M. G. and Walker, A. P. and Dietze, M. C. and Hanson, P. J. and Hickler, T. and Jain, A. K. and Luo, Y. and Parton, W. and Prentice, I. C. and Thornton, P. E. and Wang, S. and Wang, Y.-P. and Weng, E. and Iversen, C. M. and McCarthy, H. R. and Warren, J. M. and Oren, R. and Norby, R. J.: Using ecosystem experiments to improve vegetation models. Nature Clim. Change, 5, 528-534, 2015.

Medlyn, B. E., Duursma, R. A., Eamus, D., Ellsworth, D. S., Prentice, I. C., Barton, C. V. M., Crous, K. Y., De Angelis, P., Freeman, M. and Wingate, L.: Reconciling the optimal and empirical approaches to modelling stomatal conductance, Glob. Change Biol., 17, 2134–2144, 2011.

Mencuccini, M., Minunno, F., Salmon, Y., Martínez-Vilalta, J. and Hölttä, T.: Coordination of physiological traits involved in drought-induced mortality of woody plants, New Phytol., in press, 2015.

Milly, P.: Sensitivity of greenhouse summer dryness to changes in plant rooting characteristics, Geophys. Res. Lett., 24, 269–271, 1997.

Mitchell, P., O'Grady, A., Tissue, D., Worledge, D. and Pinkard, E.: Co-ordination of growth, gas exchange and hydraulics define the carbon safety margin in tree species with contrasting drought strategies, Tree Physiol., 34, 443–458, 2014.

Mitchell, P. J., O'Grady, A. P., Tissue, D. T., White, D. A., Ottenschlaeger, M. L. and Pinkard, E. A.: Drought response strategies define the relative contributions of hydraulic dysfunction and carbohydrate depletion during tree mortality, New Phytol., 197, 862–872, 2013.

Nepstad, D. C., Tohver, I. M., Ray, D., Moutinho, P. and Cardinot, G.: Mortality of large trees and lianas following experimental drought in an Amazon forest, Ecology, 88, 2259–2269, 2007.

Nepstad, D. C. and Moutinho, P. and Dias-Filho, M. B. and Davidson, E. and Cardinot, G. and Markewitz, D. and Figueiredo, R. and Vianna, N. and Chambers, J. and Ray, D. and Guerreiros, J. B. and Lefebvre, P. and Sternberg, L. and Moreira, M. and Barros, L. and Ishida, F. Y. and Tohlver, I. and Belk, E. and Kalif, K. and Schwalbe, K.: The effects of partial throughfall exclusion on canopy processes, aboveground production, and biogeochemistry of an Amazon forest, J. Geophys. Res., 107(D20), 8085, 2156-2202, 2002.

Ni, B.-R., and S. G. Pallardy. Response of gas exchange to water stress in seedlings of woody angiosperms. Tree Physiol., 8, 1–9, 1991.

Oleson, K. W., Lawrence, D. M., Bonan, G. B., Drewniak, B., Huang, M., Koven, C. D., Levis, S., Li, F., Riley, W. J., Subin, Z. M., Swenson, S. C., Thornton, P. E., Bozbiyik, A., Fisher, R., Heald, C. L., Kluzek, E., Lamarque, J.-F., Lawrence, P. J., Leung, L. R., Lipscomb, W., Muszala, S., Ricciuto, D. M., Sacks, W., Sun, Y., Tang, J. and Yang, Z.-L.: Technical Description of version 4.5 of the Community Land Model (CLM), NCAR Technical Note, Citeseer, National Center for Atmospheric Research, P.O. Box 3000, Boulder, Colarado., 2013.

Pangle, R. E., J. P. Hill, J. A. Plaut, E. A. Yepez, J. R. Elliot, N. Gehres, N. G. McDowell, and W. T. Pockman: Methodology and performance of a rainfall manipulation experiment in a piñon–juniper woodland, Ecosphere, 3, art28, 2012.

Peng, C., Ma, Z., Lei, X., Zhu, Q., Chen, H., Wang, W., Liu, S., Li, W., Fang, X. and Zhou, X.: A drought-induced pervasive increase in tree mortality across Canada's boreal forests, Nat. Clim. Change, 1, 467–471, 2011.

Phillips, O. L., Aragão, L. E. O. C., Lewis, S. L., Fisher, J. B., Lloyd, J., López-González, G., Malhi, Y., Monteagudo, A., Peacock, J., Quesada, C. A., van der Heijden, G., Almeida, S., Amaral, I., Arroyo, L., Aymard, G., Baker, T. R., Bánki, O., Blanc, L., Bonal, D., Brando, P., Chave, J., de Oliveira, Á. C. A., Cardozo, N. D., Czimczik, C. I., Feldpausch, T. R., Freitas, M. A., Gloor, E., Higuchi, N., Jiménez, E., Lloyd, G., Meir, P., Mendoza, C., Morel, A., Neill, D. A., Nepstad, D., Patiño, S., Peñuela, M. C., Prieto, A., Ramírez, F., Schwarz, M., Silva, J., Silveira, M., Thomas, A. S., Steege, H. ter, Stropp, J., Vásquez, R., Zelazowski, P., Dávila, E. A., Andelman, S., Andrade, A., Chao, K.-J., Erwin, T., Di Fiore, A., C., E. H., Keeling, H., Killeen, T. J., Laurance, W. F., Cruz, A. P., Pitman, N. C. A., Vargas, P. N., Ramírez-Angulo, H., Rudas, A., Salamão, R., Silva, N., Terborgh, J. and Torres-Lezama, A.: Drought sensitivity of the Amazon rainforest, Science, 323, 1344–1347, 2009.

962

963 Pitman, A., Avila, F., Abramowitz, G., Wang, Y., Phipps, S. and de Noblet-Ducoudré, N.:
964 Importance of background climate in determining impact of land-cover change on regional
965 climate, Nat. Clim. Change, 1, 472–475, 2011.

966

967 Powell, T. L., Galbraith, D. R., Christoffersen, B. O., Harper, A., Imbuzeiro, H. M. A.,
968 Rowland, L., Almeida, S., Brando, P. M., da Costa, A. C. L., Costa, M. H., Levine, N. M.,
969 Malhi, Y., Saleska, S. R., Sotta, E., Williams, M., Meir, P. and Moorcroft, P. R.: Confronting
970 model predictions of carbon fluxes with measurements of Amazon forests subjected to
971 experimental drought, New Phytol., 200, 350–365, 2013.

972

973 Raupach, M.: Simplified expressions for vegetation roughness length and zero-plane
974 displacement as functions of canopy height and area index, Bound.-Layer Meteorol., 71, 211–
975 216, 1994.

976

977 Raupach, M., Finkele, K. and Zhang, L.: SCAM (Soil-Canopy-Atmosphere Model):
978 Description and comparison with field data, Aspendale Aust. CSIRO CEM Tech. Rep., (132),
979 81, 1997.

980 Reich, P. B. and T. M. Hinckley. Influence of pre-dawn water potential and soil-to-leaf
981 hydraulic conductance on maximum daily leaf diffusive conductance in two oak species.
982 Funct. Ecol. 3:719-126, 1989.

983

984 Reichstein, M., Ciais, P., Papale, D., Valentini, R., Running, S., Viovy, N., Cramer, W.,
985 Granier, A., Ogée, J., Allard, V., Aubinet, M., Bernhofer, C., Buchmann, N., Carrara, A.,
986 Grünwald, T., Heimann, M., Heinesch, B., Knohl, A., Kutsch, W., Loustau, D., Manca, G.,
987 Matteucci, G., Miglietta, F., Ourcival, J. M., Pilegaard, K., Pumpanen, J., Rambal, S.,
988 Schaphoff, S., Seufert, G., Soussana, J.-F., Sanz, M.-J., Vesala, T. and Zhao, M.: Reduction of
989 ecosystem productivity and respiration during the European summer 2003 climate anomaly: a
990 joint flux tower, remote sensing and modelling analysis, Glob. Change Biol., 13, 634–651,
991 2007.

992

993 Schär, C., Vidale, P. L., Lüthi, D., Frei, C., Häberli, C., Liniger, M. A. and Appenzeller, C.:
994 The role of increasing temperature variability in European summer heatwaves, Nature, 427,
995 332–336, 2004.
996
997 Sheffield, J., Wood, E. F. and Roderick, M. L.: Little change in global drought over the past
998 60 years, Nature, 491, 435–438, 2012.
999
1000 Skelton, R. P., West, A. G. and Dawson, T. E.: Predicting plant vulnerability to drought in
1001 biodiverse regions using functional traits, 112, 5744-5749, 2015.
1002
1003 Smith, N. G., Rodgers, V. L., Brzostek, E. R., Kulmatiski, A., Avolio, M. L., Hoover, D. L.,
1004 Koerner, S. E., Grant, K., Jentsch, A. and Fatichi, S., Niyogi, D.: Toward a better integration
1005 of biological data from precipitation manipulation experiments into Earth system models,
1006 Rev. of Geophys., 52, 1944-9208, 2014.
1007
1008 Tardieu, F. and Simonneau, T.: Variability among species of stomatal control under
1009 fluctuating soil water status and evaporative demand: modelling isohydric and anisohydric
1010 behaviours, J. Exp. Bot., 49, 419–432, 1998.
1011
1012 Tyree, M., Cochard, H., Cruiziat, P., Sinclair, B. and Ameglio, T.: Drought-induced leaf
1013 shedding in walnut: evidence for vulnerability segmentation, Plant Cell Environ., 16, 879–
1014 882, 1993.
1015
1016 van Mantgem, P. J., Stephenson, N. L., Byrne, J. C., Daniels, L. D., Franklin, J. F., Fulé, P.
1017 Z., Harmon, M. E., Larson, A. J., Smith, J. M., Taylor, A. H. and others: Widespread increase
1018 of tree mortality rates in the western United States, Science, 323, 521–524, 2009.
1019
1020 Verhoef, A. and Egea, G.: Modeling plant transpiration under limited soil water: Comparison
1021 of different plant and soil hydraulic parameterizations and preliminary implications for their
1022 use in land surface models, Agric. For. Meteorol., 191, 22–32, 2014.
1023

1024 Wang, H., Prentice, I. and Davis, T.: Biophysical constraints on gross primary production by
1025 the terrestrial biosphere, Biogeosciences, 11, 5987–6001, 2014.
1026
1027 Wang, Y. P. and Leuning, R.: A two-leaf model for canopy conductance, photosynthesis and
1028 partitioning of available energy I::: Model description and comparison with a multi-layered
1029 model, Agric. For. Meteorol., 91, 89–111, 1998.
1030
1031 Wang, Y. P., Kowalczyk, E., Leuning, R., Abramowitz, G., Raupach, M. R., Pak, B., van
1032 Gorsel, E. and Luhar, A.: Diagnosing errors in a land surface model (CABLE) in the time and
1033 frequency domains, J. Geophys. Res. Biogeosciences 2005–2012, 116, 2011.
1034
1035 White, D.: Physiological responses to drought of Eucalyptus globulus and Eucalyptus nitens
1036 in plantations. PhD diss., University of Tasmania, 1996.
1037
1038 Williams, M., Rastetter, E. B., Fernandes, D. N., Goulden, M. L., Wofsy, S. C. and Shaver, G.
1039 R. and: Modelling the soil-plant-atmosphere continuum in a Quercus-Acer stand at Harvard
1040 Forest: the regulation of stomatal conductance by light, nitrogen and soil/plant hydraulic
1041 properties., Plant Cell Environ., 19, 911–927, 1996.
1042
1043 Williams, M., Bond, B. and Ryan, M.: Evaluating different soil and plant hydraulic
1044 constraints on tree function using a model and sap flow data from ponderosa pine, Plant Cell
1045 Amp Environ., 24, 679–690, 2001.
1046
1047 Woodward, F. I. and Lomas, M. R.: Vegetation dynamics - simulating responses to climate
1048 change., Biol. Rev., 79, 643–670, 2004.
1049
1050 Xu, L. and Baldocchi, D. D.: Seasonal trends in photosynthetic parameters and stomatal
1051 conductance of blue oak (Quercus douglasii) under prolonged summer drought and high
1052 temperature, Tree Physiol., 23, 865–877, 2003.
1053

Zhou, S., Duursma, R. A., Medlyn, B. E., Kelly, J. W. and Prentice, I. C.: How should we model plant responses to drought? An analysis of stomatal and non-stomatal responses to water stress, Agric. For. Meteorol., 182-183, 204–214, 2013.

Zhou, S., Medlyn, B., Sabaté, S., Sperlich, D. and Prentice, I. C.: Short-term water stress impacts on stomatal, mesophyll and biochemical limitations to photosynthesis differ consistently among tree species from contrasting climates, Tree Physiol., 10, 1035–1046, 2014.

Figure Captions

Figure 1: A comparison of the observed (OBS) and modelled (CTRL) Latent Heat (LE) and transpiration (E) at five Fluxnet sites during 2003. The data have been smoothed with a 5-day moving window to aid visualisation.

Figure 2: Modelled impact of drought on the assimilation rate (A), shown as (a) a function of volumetric soil moisture content (θ) and (b) soil water potential (Ψ_S) for a sand and clay soil.

Figure 3: A comparison of the observed (OBS) and modelled latent Heat (LE) and transpiration (E) at the Tharandt site during 2003. Simulations show the control (CTRL) and the three drought sensitivities to drought (high, medium, low) based on Zhou et al. (2013; 2014) and three different methods to calculate soil water potential (Ψ_S). The data have been smoothed with a 5-day moving window to aid visualisation.

Figure 4: A comparison of the observed (OBS) and modelled latent Heat (LE) and transpiration (E) at the Hesse site during 2003. Simulations show the control (CTRL) and the three drought sensitivities to drought (high, medium, low) based on Zhou et al. (2013; 2014) and three different methods to calculate soil water potential (Ψ_S). The data have been smoothed with a 5-day moving window to aid visualisation.

Figure 5: A comparison of the observed (OBS) and modelled latent Heat (LE) and transpiration (E) at the Roccarespampani site during 2003. Simulations show the control (CTRL) and the three drought sensitivities to drought (high, medium, low) based on Zhou et al. (2013; 2014) and three different methods to calculate soil water potential (Ψ_S). The data have been smoothed with a 5-day moving window to aid visualisation.

Figure 6: A comparison of the observed (OBS) and modelled latent Heat (LE) and

transpiration (E) at the Castelporziano Fluxnet site during 2003. Simulations show the control (CTRL) and the three drought sensitivities to drought (high, medium, low) based on Zhou et al. (2013; 2014) and three different methods to calculate soil water potential (Ψ_S). The data have been smoothed with a 5-day moving window to aid visualisation.

Figure 7: A comparison of the observed (OBS) and modelled latent Heat (LE) and transpiration (E) at the Espirra site during 2003. Simulations show the control (CTRL) and the three drought sensitivities to drought (high, medium, low) based on Zhou et al. (2013; 2014) and three different methods to calculate soil water potential (Ψ_S). The data have been smoothed with a 5-day moving window to aid visualisation.

Supplementary Figure 1: Simulated soil water content of each of CABLE's six layers for the control (CTRL), and three drought sensitivities (high, medium, low) based on Zhou et al. (2013; 2014) at the Tharandt site. The grey shading highlights the heatwave period between the 1st of June and the 31st of August. The data have been smoothed with a 5-day moving window to aid visualisation.

Supplementary Figure 2: Simulated soil water content of each of CABLE's six layers for the control (CTRL), and three drought sensitivities (high, medium, low) based on Zhou et al. (2013; 2014) at the Hesse site. The grey shading highlights the heatwave period between the 1st of June and the 31st of August. The data have been smoothed with a 5-day moving window to aid visualisation.

Supplementary Figure 3: Simulated soil water content of each of CABLE's six layers for the control (CTRL), and three drought sensitivities (high, medium, low) based on Zhou et al. (2013; 2014) at the Roccarespampani site. The grey shading highlights the heatwave period between the 1st of June and the 31st of August. The data have been smoothed with a 5-day moving window to aid visualisation.

Supplementary Figure 4: Simulated soil water content of each of CABLE's six layers for the control (CTRL), and three drought sensitivities (high, medium, low) based on Zhou et al. (2013; 2014) at the Castelporziano site. The grey shading highlights the heatwave period between the 1st of June and the 31st of August. The data have been smoothed with a 5-day moving window to aid visualisation.

Supplementary Figure 5: Simulated soil water content of each of CABLE's six layers for the control (CTRL), and three drought sensitivities (high, medium, low) based on Zhou et al. (2013; 2014) at the Espirra site. The grey shading highlights the heatwave period between the 1st of June and the 31st of August. The data have been smoothed with a 5-day moving window to aid visualisation.

Table 1. Baseline parameter values used to represent the three sensitivities: "high" (*Quercus robur*), "medium" (*Quercus ilex*) and "low" (*Cedrus atlantica*) to drought stress. Paramater values are taken from Zhou et al. (2013; 2014).

Sensitivity	b	S_f	Ψ_f
High	1.55	6.0	–0.53
Medium	0.82	1.9	–1.85
Low	0.46	5.28	–2.31

Table 2: Summary of flux tower sites.

Site	PFT	Dominant species	Latitude	Longitude	Country	Sand/Silt/Clay Fraction
Tharandt	ENF	*Picea abies*	50°58' N	13°34' E	Germany	0.37/0.33/0.3
Hesse	DBF	*Fagus sylvatica*	48°40' N	7°05' E	France	0.37/0.33/0.3
Roccarespampani	DBF	*Quercus cerris*	42°24' N	11°55' E	Italy	0.6/0.2/0.2
Castelporziano	EBF	*Quercus ilex*	41°42' N	12°22' E	Italy	0.6/0.2/0.2
Espirra	EBF	*Eucalyptus globulus*	38°38' N	8°36' W	Portugal	0.37/0.33/0.3

1165 Table 3: Mean change in climate and fluxes between 2002 and 2003 covering the period
1166 between June and September.

Site	Precipitation (mm month^{-1})	Air temperature (° C)	GPP (g C m^{-2} month^{-1})	LE (W m^{-2})
Tharandt	-115.57	1.45	-38.45	0.52
Hesse	-49.20	2.98	-123.38	-11.90
Roccarespampani	-87.36	2.18	-71.94	-6.17
Castelporziano	-20.31	4.57	-49.73	-6.47
Espirra	-14.45	1.77	28.46	22.83

1167

1168

1169

1170

1171

1172 Table 4: Summary statistics of modelled and observed LE at the five FLUXNET sites during the main drought period (1st of June – 31st
1173 August, 2003). For each site the best performing model simulation has been highlighted in bold.

Site	Ψ_S Method	Root Mean Squared Error (RMSE; W m^{-2})				Nash-Sutcliffe efficiency (NSE)				Pearsons's correlation coefficient (r)			
		CTRL	High	Medium	Low	CTRL	High	Medium	Low	CTRL	High	Medium	Low
Tharandt	1	21.25	24.64;	26.57	29.55	-0.70	-1.28	-1.65	-2.28	0.69	**0.73**	**0.73**	0.70
	2		34.59	36.20	36.97		-3.50	-3.93	-4.14		0.58	0.56	0.55
	3		**25.90**	29.39	32.26		**-1.52**	-2.25	-2.94		0.72	0.67	0.63
Hesse	1	28.50	36.22	41.59	51.49	0.15	-0.37	-0.81	-1.77	0.68	0.66	0.74	0.79
	2		52.60	59.87	63.46		-1.89	-2.75	-3.21		0.80	0.75	0.71
	3		**28.82**	45.32	56.46		**0.13**	-1.15	-2.33		0.79	**0.84**	0.77
Roccarespampani	1	38.00	48.41	40.98	34.27	-0.34	-1.17	-0.55	-0.09	0.67	0.52	0.67;	0.81
	2		31.62	22.81	26.81		0.08	0.52	0.34		0.83	0.84;	0.79
	3		45.12	**18.27**	29.50		-0.88	**0.69**	0.20		0.67	**0.85**	0.81
Castelporziano	1	31.76	38.77	40.54	40.40	-8.95	-13.82	-15.21	-15.10	0.18	-0.08	0.01	0.06
	2		31.04	27.19	**19.72**		-8.50	-6.29	**-2.84**		0.47	0.54	0.57
	3		39.17	20.47	20.41		-14.40;	-3.13	-3.11		-0.02	0.55	**0.61**
Espirra	1	35.31	41.52	40.97	33.87	-3.35	-5.02;	-4.86	-3.01;	0.42	0.32	0.59	0.70
			15.58	**13.82**	**13.84**		0.15	**0.33**	**0.33**		**0.77**	**0.74**	0.73

1174

1175 Table 5: Summary statistics of modelled and observed GPP at the five FLUXNET sites during the main drought period (1st of June – 31st
1176 August, 2003). For each site the best performing model simulation has been highlighted in bold.

Site	Ψ_S Method	Root Mean Squared Error (RMSE; g C m^{-2} d^{-1})				Nash-Sutcliffe efficiency (NSE)				Pearsons's correlation coefficient (r)			
		CTRL	High	Medium	Low	CTRL	High	Medium	Low	CTRL	High	Medium	Low
Tharandt	1	2.06	2.27	**2.07**	2.10	0.33	0.19	**0.33**	0.31	0.80	**0.71**	0.66	0.61
	2		2.25	2.29	2.30		0.20	0.18	0.17		0.52	0.51	0.50
	3		2.23	2.12	2.20		0.22	0.30	0.25		0.66	0.59	0.55
Hesse	1	2.85	3.57	**2.48**	2.94	0.48	0.18	**0.60**	0.44	0.79	0.78	0.78	0.71
	2		2.65	3.22	3.47		0.55	0.33	0.22		0.75	0.67	0.62
	3		3.51	2.71	3.24		0.21	0.53	0.32		**0.83**	0.75	0.66
Roccarespampani	1	2.49	3.70	2.69	2.38	0.42	-0.28	0.32	0.47	0.85	0.64	0.82	0.87
	2		2,12	**1.47**	2.84		0.58	**0.80**	0.24		**0.92**	0.91	0.87
	3		3.74	1.73	3.08		-0.31	0.72	0.11		0.84	0.91	0.85
Castelporziano	1	2.22	3.46	3.64	3.76	-2.16	-6.71	-7.51	-8.08	0.55	-0.18	0.07	0.13
	2		2.65;	1.84	1.22		-3.52	-1.17	0.04		0.63	0.63	**0.81**
	3		3.71	**0.95**	1.46		-7.82	**0.42**	-0.37		0.05	**0.81**	0.84
Espirra	1	3.03	4.39	4.33	3.72	-2.67	-6.72	-6.51	-4.55	0.74	0.58	0.53	0.67
	2		1.92	1.46	**1.34**		-0.48	0.14	**0.28**		0.80	**0.81**	**0.81**
	3		4.70	2.01	1.43		-7.84	-0.62	0.18		0.34	0.74	0.78

1177

Figure 1

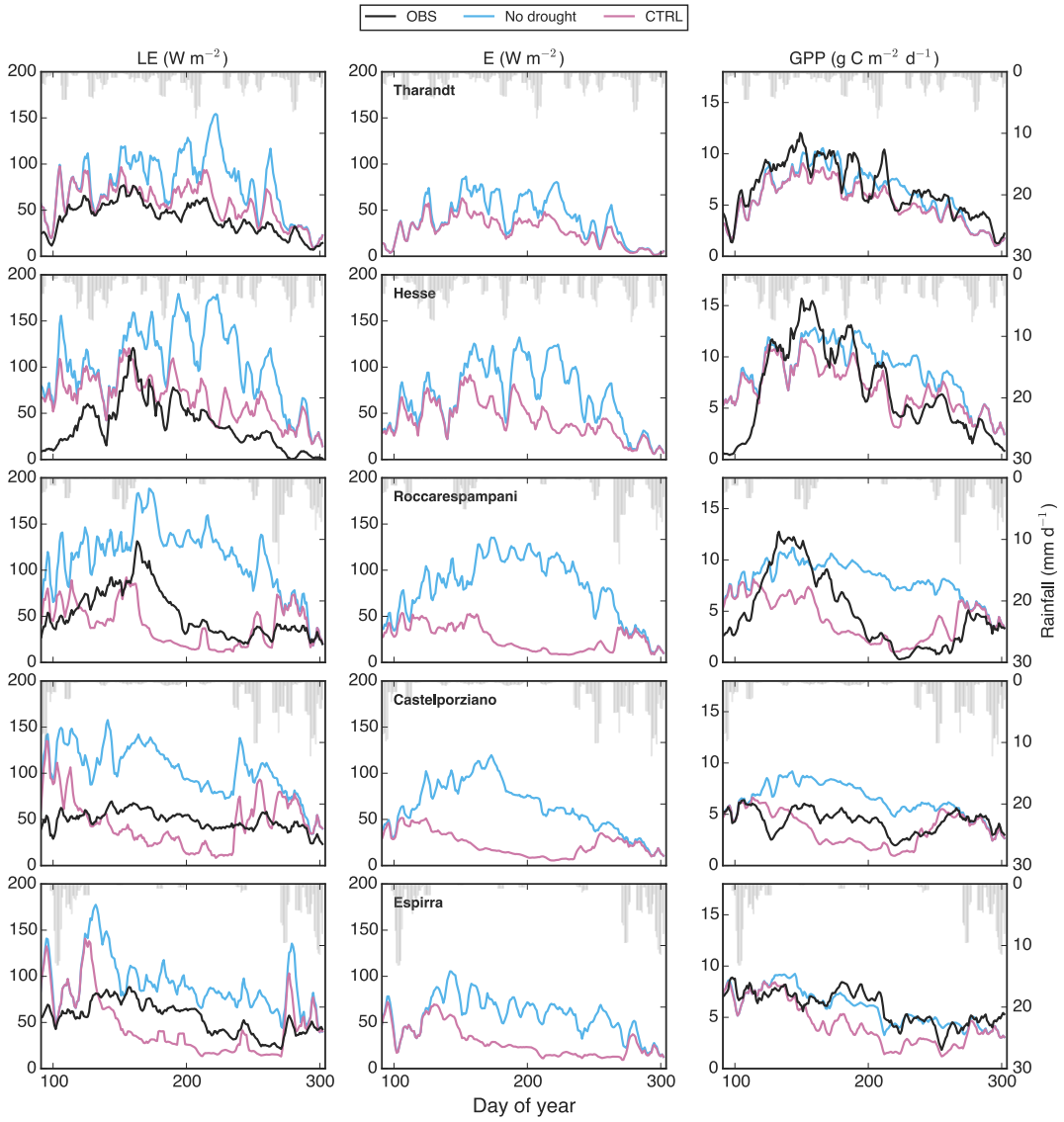
OBS
No drought
CTRL
LE (W m^{-2})
E (W m^{-2})
GPP (g C m^{-2} d^{-1})
Tharandt
Hesse
Roccarespampani
Castelporziano
Espirra
Rainfall (mm d^{-1})
Day of year

Figure 2

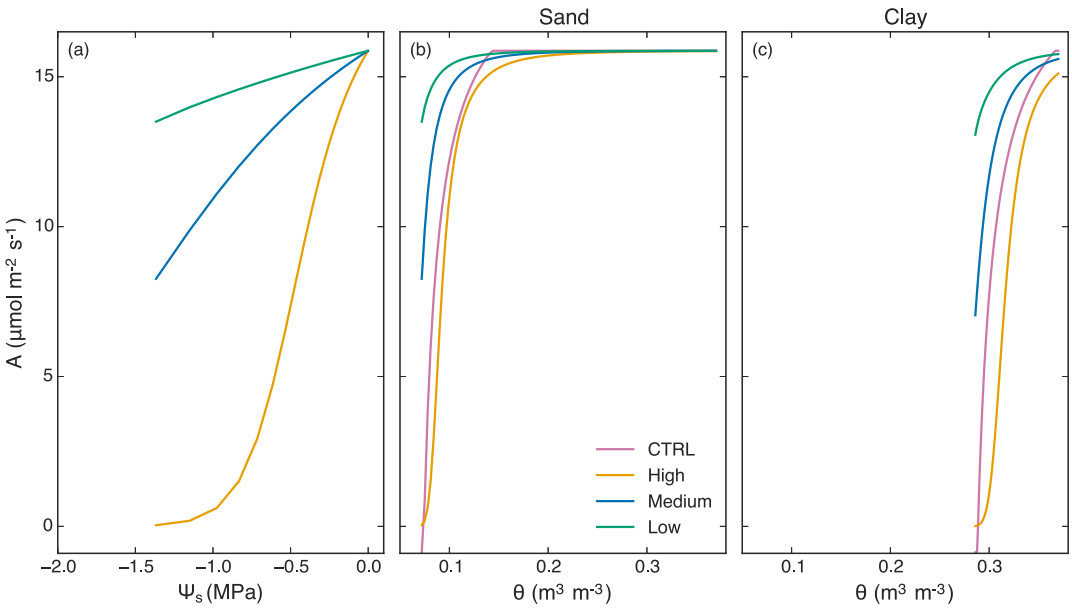
Sand
Clay
(a)
(b)
(c)
A (µmol m-2 s-1)
15
10
5
0
−2.0
−1.5
−1.0
−0.5
0.0
Ψs (MPa)
0.1
0.2
0.3
θ (m3 m-3)
CTRL
High
Medium
Low

Figure 3

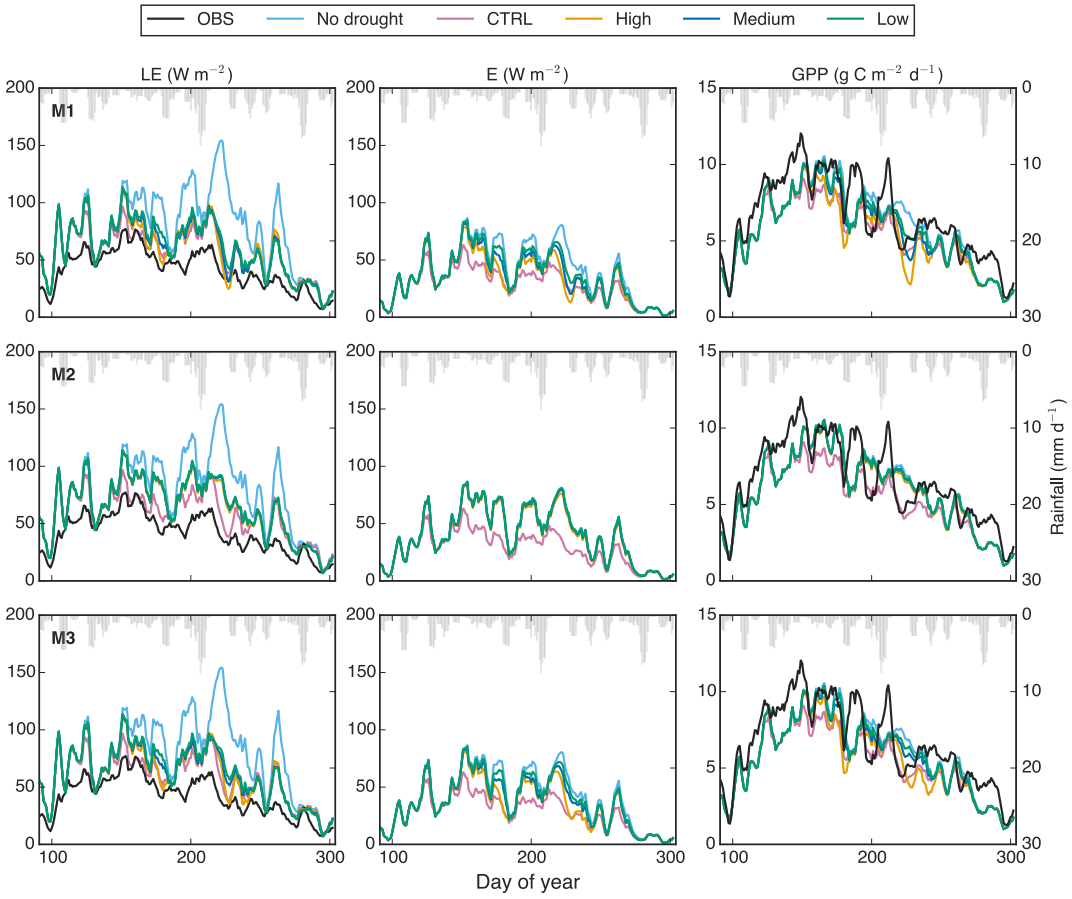
OBS
No drought
CTRL
High
Medium
Low
LE (W m^{-2})
E (W m^{-2})
GPP (g C m^{-2} d^{-1})
M1
M2
M3
Rainfall (mm d^{-1})
Day of year

Figure 4

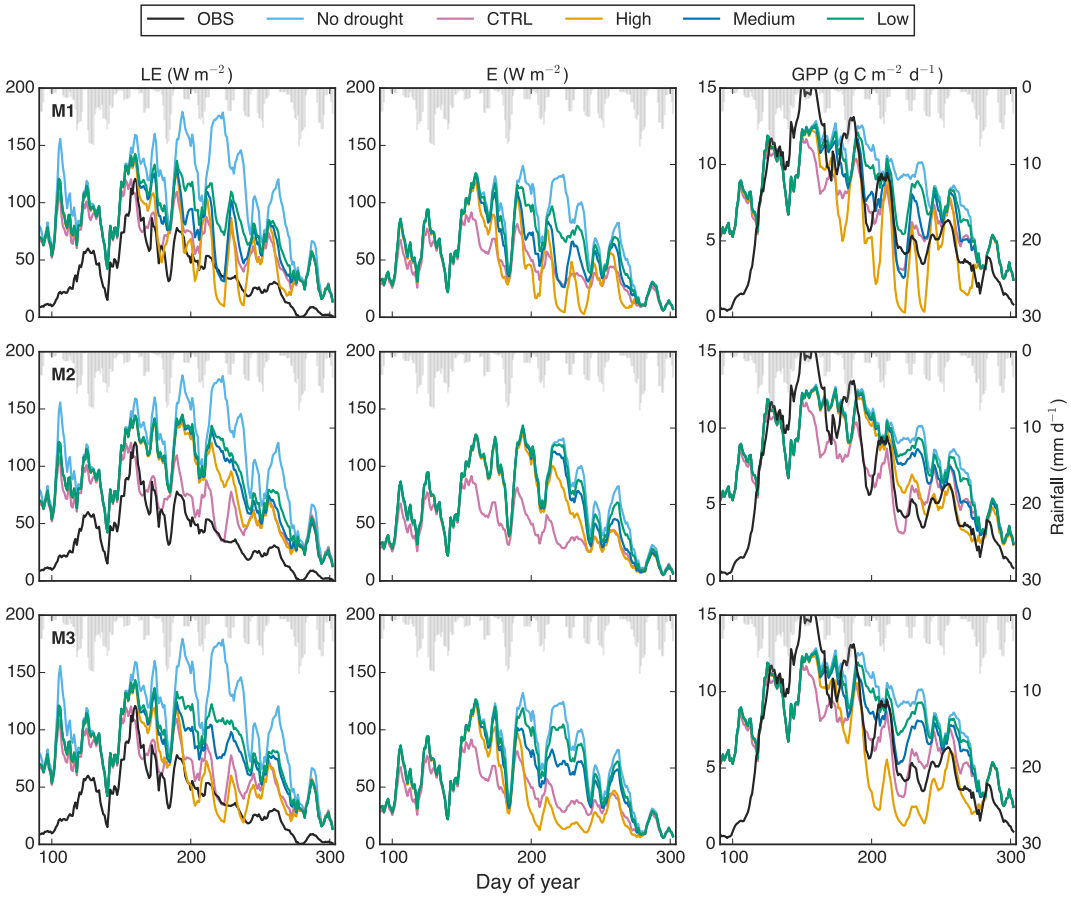
OBS
No drought
CTRL
High
Medium
Low
LE (W m^{-2})
E (W m^{-2})
GPP (g C m^{-2} d^{-1})
M1
M2
M3
Rainfall (mm d^{-1})
Day of year

Figure 5

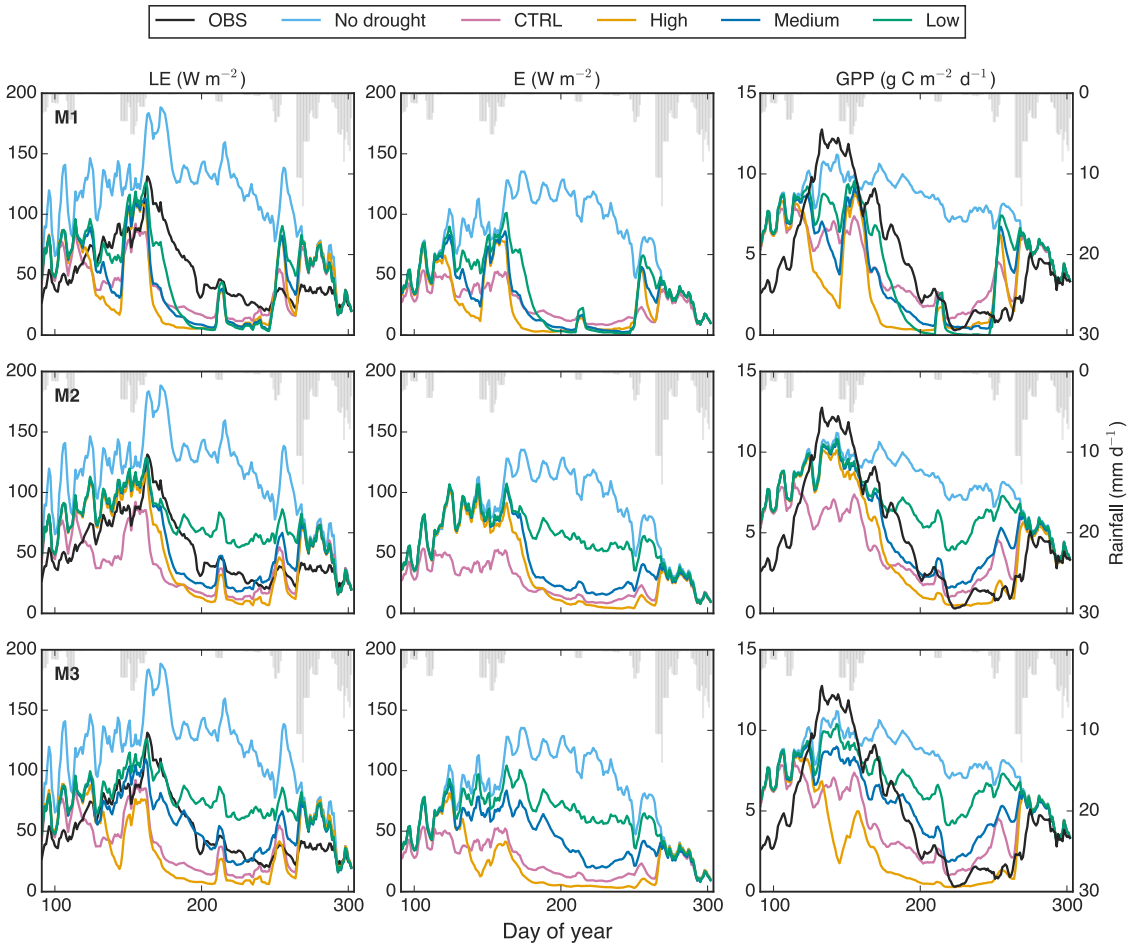
OBS
No drought
CTRL
High
Medium
Low
LE (W m^{-2})
E (W m^{-2})
GPP (g C m^{-2} d^{-1})
M1
M2
M3
Rainfall (mm d^{-1})
Day of year

Figure 6

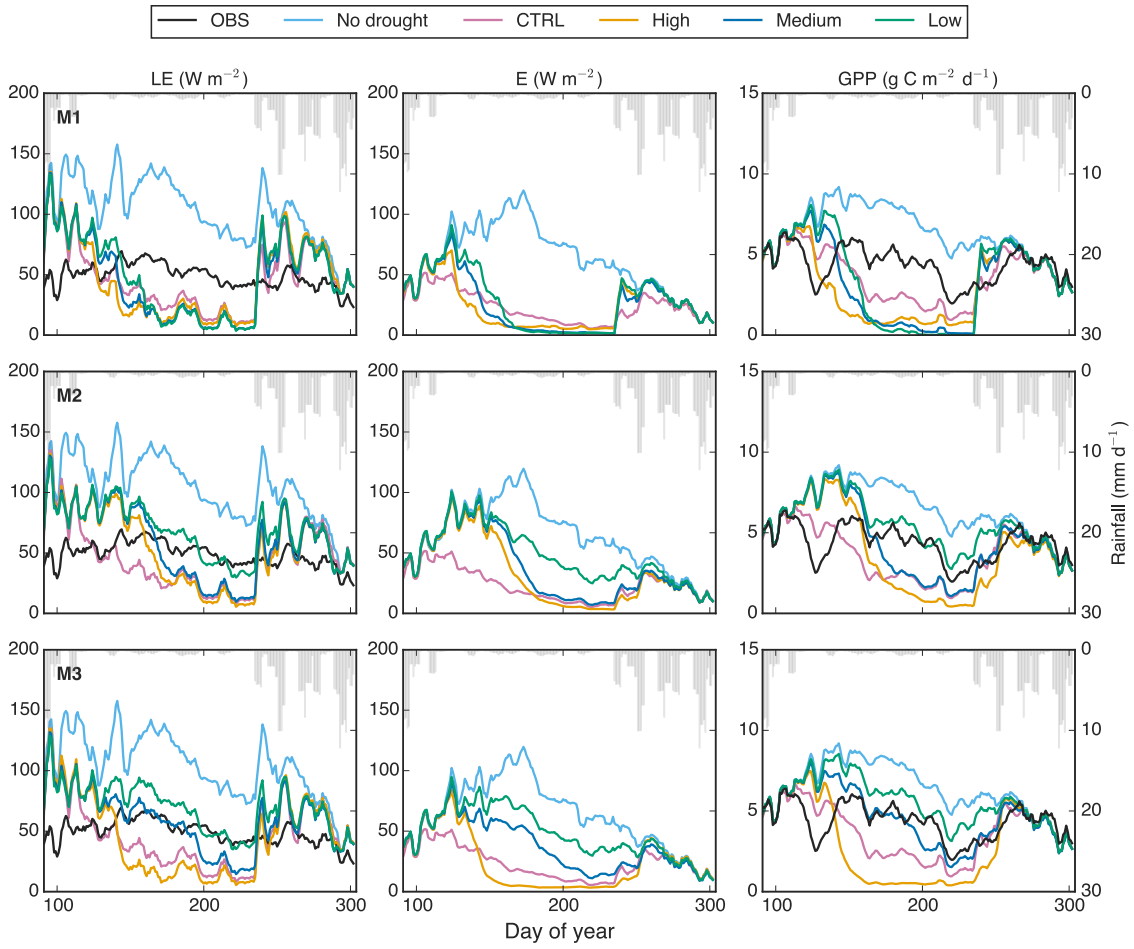
OBS
No drought
CTRL
High
Medium
Low
LE (W m^{-2})
E (W m^{-2})
GPP (g C m^{-2} d^{-1})
M1
M2
M3
Rainfall (mm d^{-1})
Day of year

Figure 7

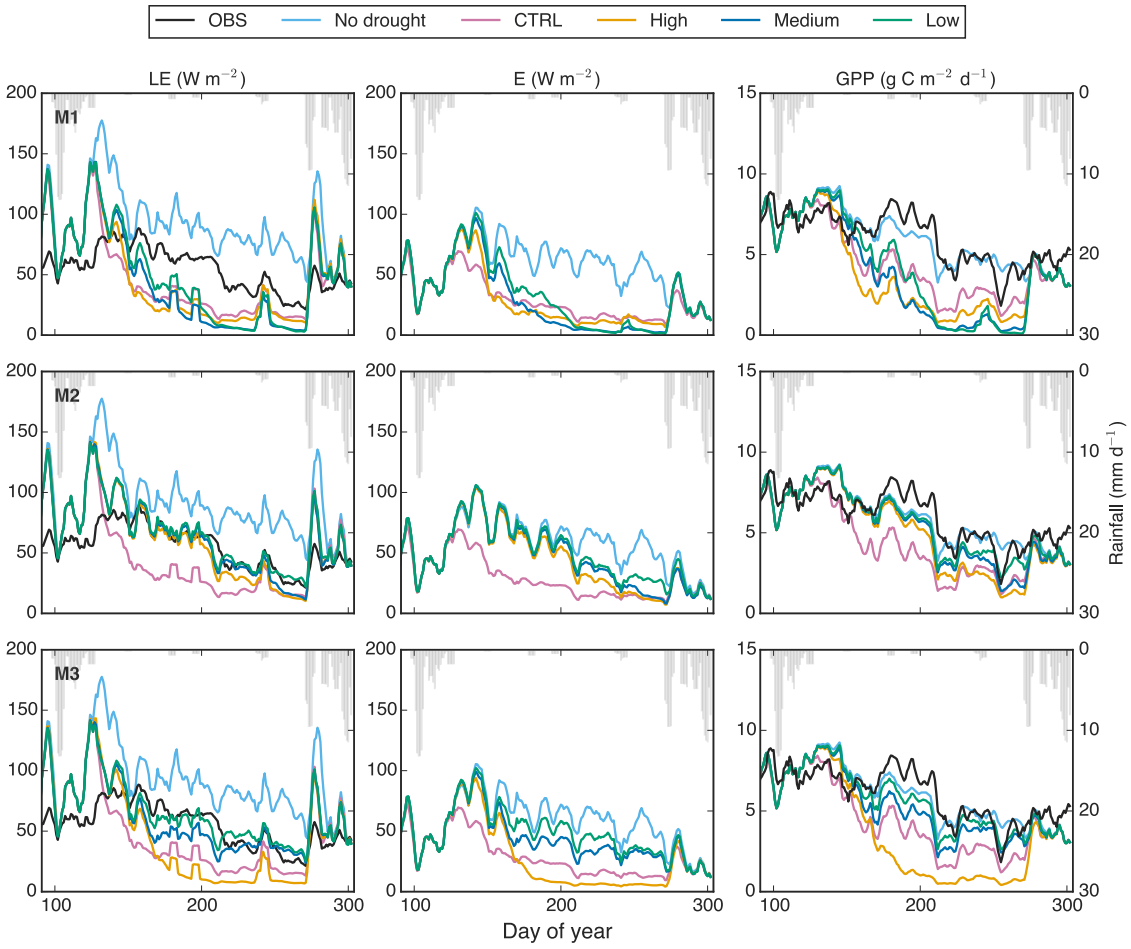
OBS
No drought
CTRL
High
Medium
Low
LE (W m^{-2})
E (W m^{-2})
GPP (g C m^{-2} d^{-1})
M1
M2
M3
Rainfall (mm d^{-1})
Day of year

Figure S1

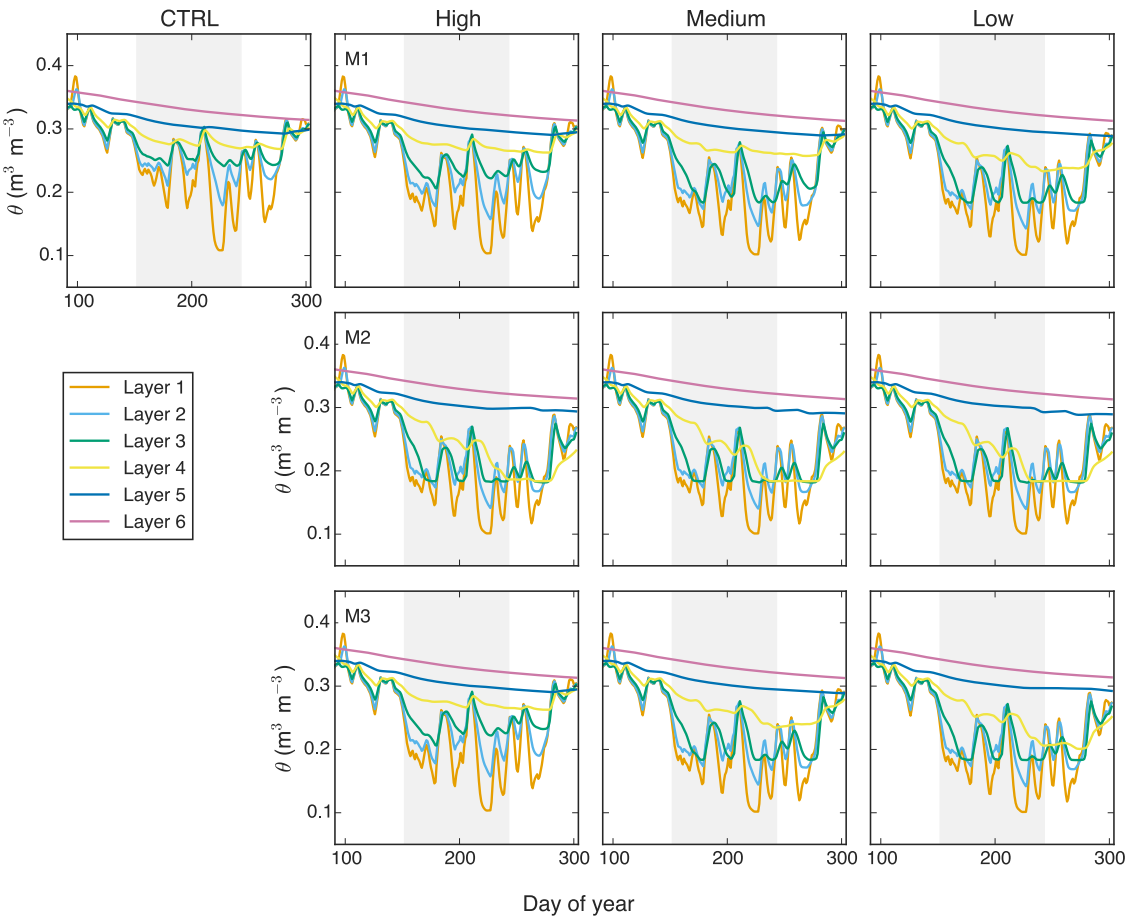
CTRL
High
Medium
Low
M1
M2
M3
θ (m³ m⁻³)
0.4
0.3
0.2
0.1
100
200
300
Layer 1
Layer 2
Layer 3
Layer 4
Layer 5
Layer 6
Day of year

Figure S2

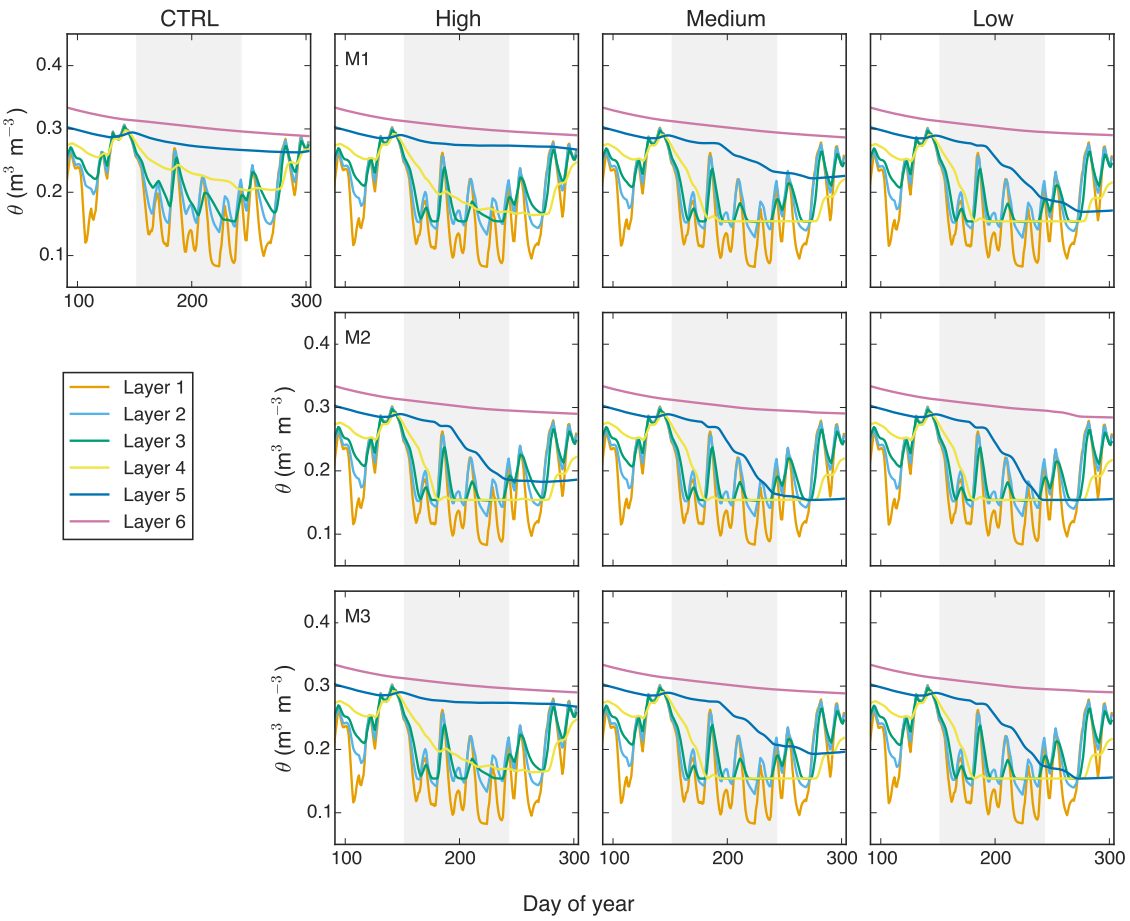
CTRL
High
Medium
Low
M1
M2
M3
θ (m³ m⁻³)
0.4
0.3
0.2
0.1
100
200
300
Layer 1
Layer 2
Layer 3
Layer 4
Layer 5
Layer 6
Day of year

Figure S3

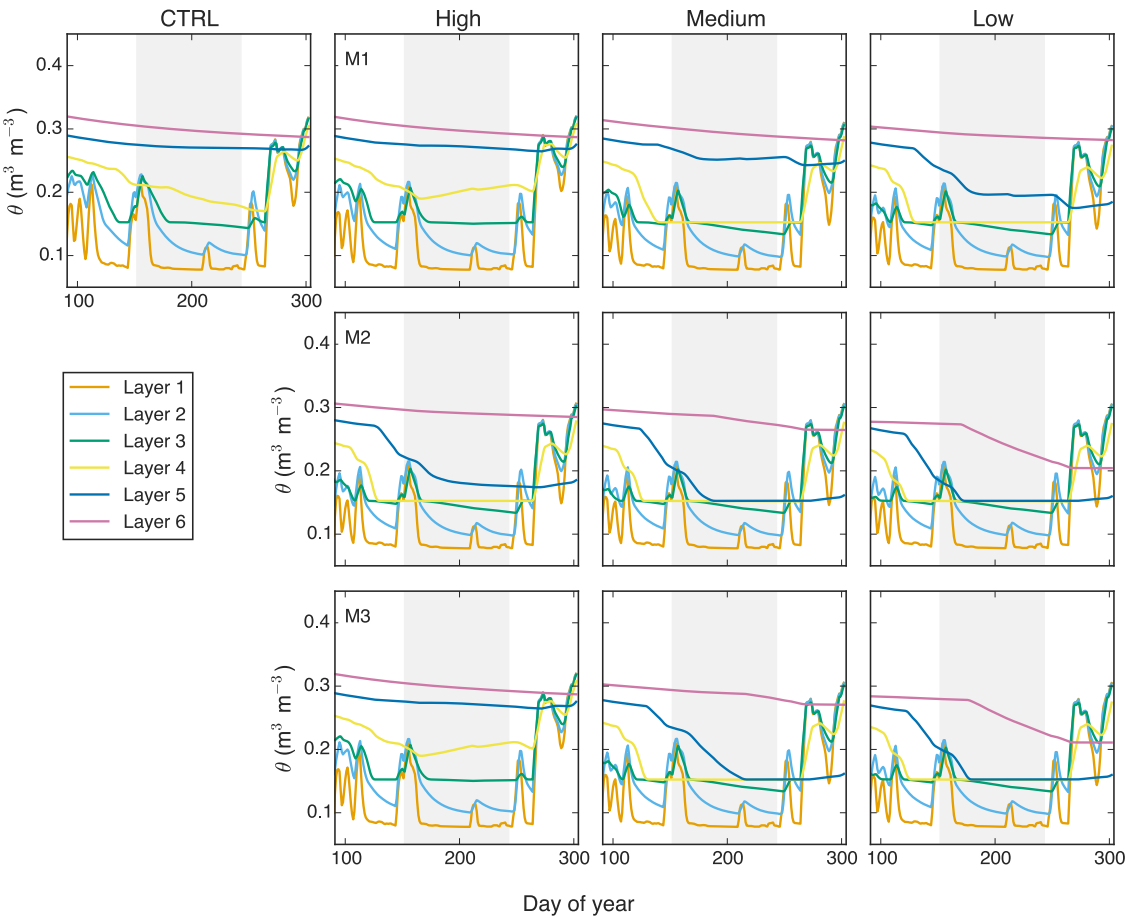
CTRL
High
Medium
Low
M1
M2
M3
θ (m³ m⁻³)
0.4
0.3
0.2
0.1
100
200
300
Layer 1
Layer 2
Layer 3
Layer 4
Layer 5
Layer 6
Day of year

Figure S4

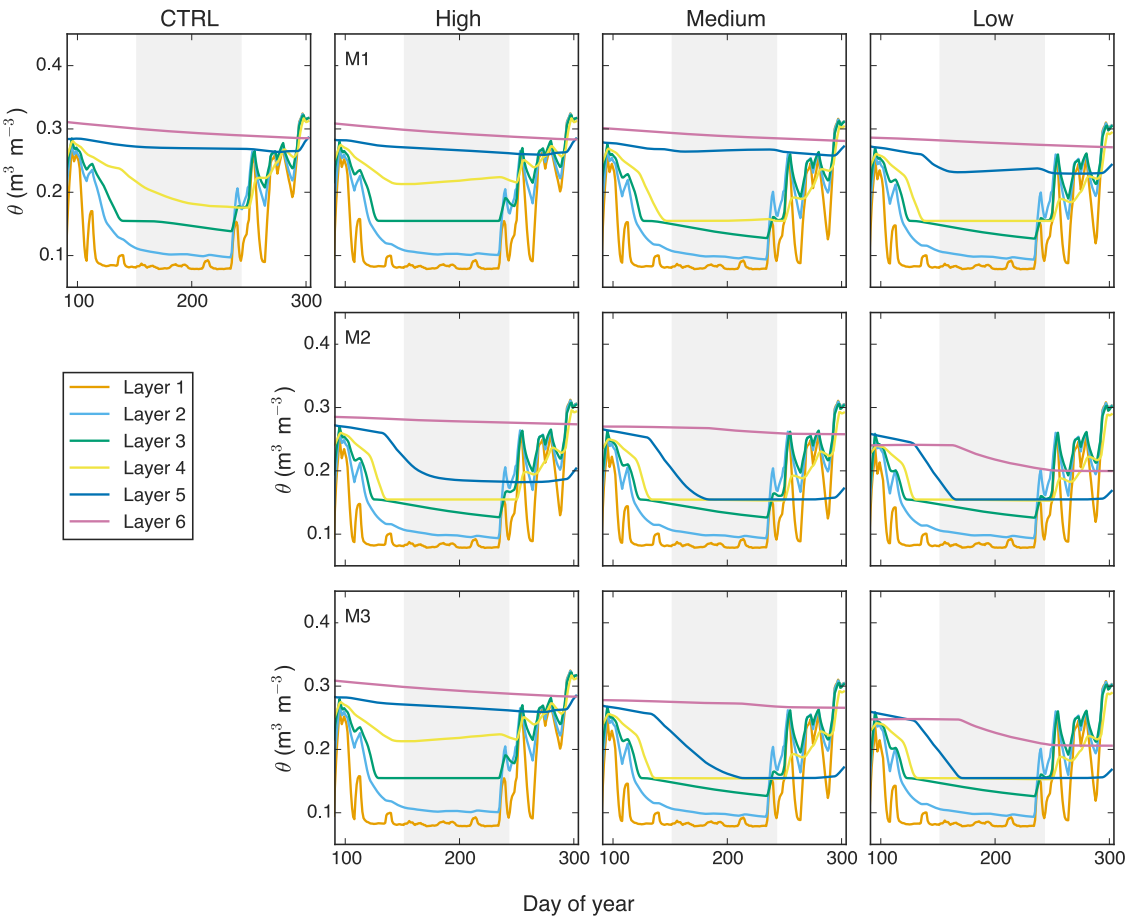
CTRL
High
Medium
Low
M1
M2
M3
θ (m³ m⁻³)
0.4
0.3
0.2
0.1
100
200
300
Layer 1
Layer 2
Layer 3
Layer 4
Layer 5
Layer 6
Day of year

Figure S5

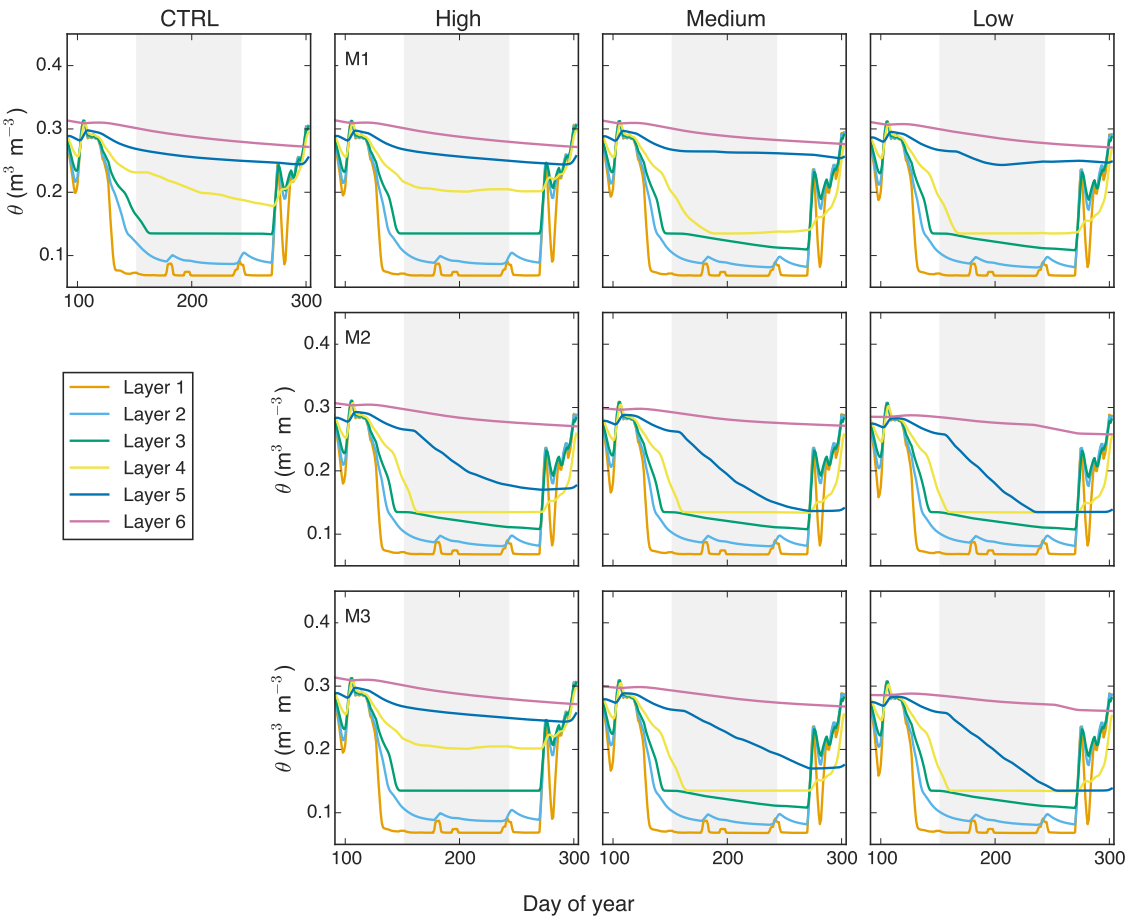
CTRL
High
Medium
Low
M1
M2
M3
θ (m³ m⁻³)
0.4
0.3
0.2
0.1
100
200
300
Layer 1
Layer 2
Layer 3
Layer 4
Layer 5
Layer 6
Day of year